Applications of Perfect Difference Codes in Fiber-optics and Wireless Optical Code-Division Multiplexing/Multiple-Access Systems

Fahim Aziz Umrani

Faculty of Advanced Technology
University of Glamorgan

A thesis submitted to the University of Glamorgan
in fulfillment of the requirement for the degree of
Doctor of Philosophy

December 2009

Dedicated to my parents

Shehar Bano (Mother) & Abdul Aziz Umrani (Father)

Certificate of Originality

I hereby certify that the work embodied in this thesis is the result of original research and that appropriate credit has been given where reference has been made to the work of others and that it has not been submitted for a higher degree to any other university or institution.

_____   _____

Date   Fahim Aziz Umrani

ACKNOWLEDGEMENTS

Praise be to God, the most gracious and the most merciful. Without His blessings and guidance our accomplishments would never have been possible. The author wishes to express his deepest gratitude to his supervisor, Prof. Dr. S. S. A. Obayya for his invaluable encouragement, support and guidance throughout the project.

The author would also like to extend his sincere thanks to Mehran University of Engineering & Technology, Pakistan and University of Glamorgan, United Kingdom for their financial support.

I gratefully acknowledge all my former and present colleagues and staff at the Faculty of Advanced Technology, Photonic Research Group, Room 356 for creating such a friendly and pleasant environment. I will never forget the formal and informal meetings which we used to have at Room 356 regularly.

Finally, I would like to thank my parents, family especially to my brothers and sisters and to my friends for their unfailing support and belief in me. Without their prayers and support this thesis would have never been completed.

Table of Contents

LIST OF FIGURES

List of Tables

LIST OF ABBREVIATIONS

APD	Avalanche Photodiode
AWG	Arrayed Waveguide Grating
BER	Bit Error Rate
BPSK	Binary Phase Shift Keying
CDMA	Code-Division Multiple-Access
CSIK	Complementary SIK
CSMA/CD	Carrier-Sense Multiple-Access/Collision Detection
DFE	Decision Feedback Equalizer
DWDM	Dense Wavelength Division Multiplexing
EDFA	Erbium Doped Fiber Amplifier
EIRP	Equivalent Isotropically Radiated Power
FCC	Federal Communication Commission
FDMA	Frequency Division Multiple Access
FO-CDMA	Fiber Optic – CDMA
FO-LAN	Fiber Optic – Local Area Network
FOV	Field of View
ICI	Inter-Chip Interference
IM/DD	Intensity Modulation/Direct Detection
IR	Infrared
ISI	Inter-Symbol Interference
LOS	Line of Sight

MAI	Multiple Access Interference
MBOK	M-ary bi-orthogonal keying
MCWC	Manchester-coded Walsh Codes
MCMLC	Manchester-coded Modified Legendre Sequences
MUX	Multiplexer
OBI	Optical Beating Interference
OCDMA	Optical CDMA
OMAN	Optical Multiple-Access Network
OOC	Optical Orthogonal Code
OOK	On-Off Keying
PAN	Personal Area Networks
PDC	Perfect Difference Codes
PIN	Positive-Intrinsic-Negative
PIIN	Phase-induced Intensity noise
PPM	Pulse Position Modulation
QoS	Quality of Service
SAC	Spectral Amplitude Coding
SAE	Spectral Amplitude Encoding
SIK	Sequence Inverse Keying
SNR	Signal to Noise Ratio
SPE	Spectral Phase Encoding
SOA	Semiconductor Optical Amplifier
TC	Turbo Coding

TDMA   Time Division Multiple Access

WDMA   Wavelength Division Multiple Access

WIR   Wireless Infrared

WLAN   Wireless LAN

List of Symbols

b_0 is the desired bit

B is the electrical bandwidth of the receiver,

e is the electron charge,

f is the optical frequency

F_e is the excess noise factor,

F_i is the set of all possible $\vec{\phi}$

G_1 is the average APD gain,

$G(v)$ is the single sideband power spectral density (PSD) of the source

h is the Planck's constant,

I Number of interfering users

I_b is the bulk leakage current,

I_p is the photocurrent,

I_s is the surface leakage current,

K_b is the Boltzmans constant,

ls is the uniformity loss in splitters in dB

N number of active users is

P is the input power,

Pe is the Probability of Error

P_r is the received power

R_L is the load resistance

T_b is the bit duration,

T_c is the chip duration,

T_n is the receiver noise temperature, and

v is the length of the code

w is the weight of the code

λ is the average photon arrival rate

η is the APD quantum efficiency

γ cross-correlation constraint

θ is the Threshold

ϕ is the vector of received interference

σ_{th} is the variance of thermal noise

τ is the source coherence time

Δv is the bandwidth of the receiver

ABSTRACT

After establishing itself in the radio domain, Spread spectrum code-division multiplexing/multiple-access (CDMA) has seen a recent upsurge in optical domain as well. Due to its fairness, flexibility, service differentiation and increased inherent security, CDMA is proved to be more suitable for the bursty nature of local area networks than synchronous multiplexing techniques like Frequency/Wavelength Division Multiplexing (F/WDM) and Time Division Multiplexing (TDM). In optical domain, CDMA techniques are commonly known as Optical-CDMA (O-CDMA). All optical CDMA systems are plagued with the problem of multiple-access interference (MAI). Spectral amplitude coding (SAC) is one of the techniques used in the literature to deal with the problem of MAI. The choice of spreading code in any CDMA system is another way to ensure the successful recovery of data at the receiving end by minimizing the effect of MAI and it also dictates the hardware design of the encoder and decoder.

This thesis focuses on the efficient design of encoding and decoding hardware. Perfect difference codes (PDC) are chosen as spreading sequences due to their good correlation properties. In most of the literature, evaluation of error probability is based on the assumptions of ideal conditions. Such assumptions ignore major physical impairments such as power splitting losses at the multiplexers of transmitters and receivers, and gain losses at the receivers, which may in practice be an overestimate or underestimate of the actual probability of error.

This thesis aims to investigate thoroughly with the consideration of practical impairments the applications of PDCs and other spreading sequences in optical communications systems based on spectral-amplitude coding and utilizing code-division as multiplexing/multiple-access technique. This work begins with a

general review of optical CDMA systems. An open-ended practical approach has been used to evaluate the actual error probabilities of OCDM/A systems under study. It has been concluded from results that mismatches in the gains of photodetectors, namely avalanche photodiode (APDs), used at the receiver side and uniformity loss in the optical splitters results in the inaccurate calculation of threshold level used to detect the data and can seriously degrade the system bit error rate (BER) performance. This variation in the threshold level can be compensated by employing techniques which maintain a constant interference level so that the decoding architecture does not have to estimate MAI every time to make a data bit decision or by the use of balanced sequences.

In this thesis, as a solution to the above problem, a novel encoding and decoding architecture is presented for perfect difference codes based on common zero code technique which maintains a constant interference level at all instants in CDM system and thus relieves the need of estimating interference. The proposed architecture only uses single multiplexer at the transmitters for all users in the system and a simple correlation based receiver for each user. The proposed configuration not only preserves the ability of MAI in Spectral-Amplitude Coding SAC-OCDM system, but also results in a low cost system with reduced complexity. The results show that by using PDCs in such system, the influence of MAI caused by other users can be reduced, and the number of active users can be increased significantly.

Also a family of novel spreading sequences are constructed called Manchester-coded Modified Legendre codes (MCMLCs) suitable for SAC based OCDM systems. MCMLCs are designed to be used for both single-rate and Multirate systems. First the construction of MCMLCs is presented and then the bit error rate performance is analyzed.

Finally the proposed encoding/decoding architecture utilizing perfect difference codes is applied in wireless infrared environment and the performance is found to be superior to other codes.

1. Introduction

1.1 Overview

Spread spectrum code-division multiple-access (CDMA) is used in both radio frequency (RF) and optical domain. It is proved to be more suitable for the bursty nature of local area networks than synchronous multiplexing techniques like FDM, TDM and WDM and is being considered as a natural solution to provide asynchronous, high-speed connectivity in the local area networks [1]. Optical code division multiple access (O-CDMA) techniques have been developed for almost two decades, first applied by Pruncal, Salehi and others [2, 3], and have emerged as attractive schemes for optical networks due to their fairness, flexibility, simplified network control and management, service differentiation and increased inherent security. The huge pool of bandwidth available in the optical medium is efficiently exploited by the CDMA, which results in better spectral efficiency, and higher throughput with no waiting.

In optical CDMA systems, each user's optical signal is encoded optically in an optical encoder that maps each bit into a very high rate optical sequence, substantially increasing the bandwidth occupied by the transmitted signal.

Figure 1.1 shows the encoding of the data bit sequence '101' using on-off keying (OOK) scheme by unipolar CDMA sequence '10010'. The data bit '1' is represented by the presence of optical pulses and '0' by the absence of the pulses. The pulses are mapped according to the assigned optical sequence. The number of ones or pulses in a code is called the *weight* (w) of the code. In Figure 1.1, T_b indicates the bit duration and T_c the chip duration. Temporal length (v) is equal to the number of chips in a sequence and is given by $v = T_b / T_c$. The limited availability of suitable orthogonal codes restricts the total number of users in an optical CDMA system.
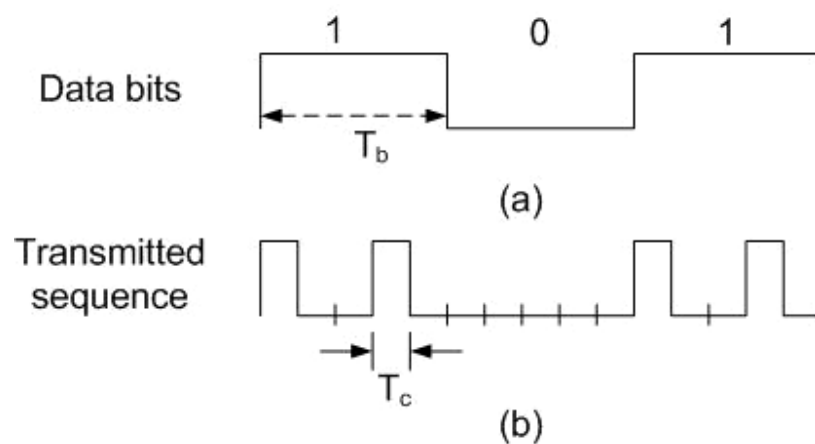
Figure 1-1: Encoding in optical CDMA (a) data bits '101' (b) transmitted sequence 10010 for bit '1'

Therefore, to support many subscribers, a large set of code sequences is needed, which implies that very narrow pulses have to be used. The encoded optical

signals from all active users are broadcasted in the network by a star coupler. At the receiver, the optical decoder is matched to the transmitting node giving a high auto-correlation peak and low cross-correlation function, only if the appropriate code was used. Hence, the desired user's transmitted signal is detected by the photodetector. All other received signals other than the desired users are termed as *multiple access interference* (MAI).

The choice of spreading code is critical to any CDMA based system. Without appropriate spreading sequence the successful recovery of the data at the receiving end would be impossible. Furthermore, it also dictates the hardware design of the encoder and decoder. Therefore, the two requirements which must be satisfied by the optical codes for any CDMA based communication system are:

1. The code must have high auto-correlation and low cross-correlation function.

2. The design of encoders and decoders to implement these codes must not be complex.

Recently, the use of perfect difference codes (PDC) has been reported for both synchronous [4] and asynchronous [5] optical CDMA based systems based on spectral amplitude coding. The detailed description of Perfect difference codes is discussed in the next chapter.

In [5], it is reported that the use of PDC can result in high-capacity high-data rate asynchronous operation of FO-LAN with relatively easy implementation of

encoders and decoders using array-waveguide (AWG) multiplexers. Such attractive feature of PDC promotes the thorough investigation of applications of such codes in both fiber optics and wireless optical communication systems.

1.2 Motivation

While the performance of long-distance Dense-Wavelength Division Multiplexing (DWDM) systems is announced in terabits per second, most of us continue to use networks whose aggregate capacities are 10 or 100 Mb/s. Each user may well require individual data rates in gigabits per second, leading to aggregate data rates reaching hundreds of gigabits per second. Moreover, such network must also provide quality of service (QoS) guarantees for these applications, even as the number of users and aggregate throughput change with time.

In this particular environment, Optical CDMA offers an interesting alternative for LANs as compared to traditional LAN multiple-accessing techniques, namely TDMA and WDMA, because neither time nor frequency management of all nodes is necessary [1]. Optical CDMA results in very low latencies because it liberates the network from synchronization, and as dedicated time or wavelength slots do not have to be allocated, the statistical multiplexing gains can be high. CDMA also allows flexible network design because the bit error rate (BER) depends on the number of active users. The new users can be accommodated in the system simply by utilizing spreading sequences with larger cardinality (i.e., soft-limited).

4

However, several challenging points of research are still missing for practical OCDMA realization and development. These include:

- The high Multiple Access Interference (MAI) which is naturally present in almost all forms of OCDMA,

- Increasing network capacity in terms of number of concurrent users, and

- Codes that can support various traffic demands in terms of bandwidth and Bit Error Rate (BER) performance. Furthermore, it is logical to search for new OCDMA implementations that can meet the expected performance requirements in a simple and cost effective way.

1.3 Scope of the Thesis

The main aim of this work is to thoroughly investigate the applications of perfect difference codes (PDC) in fiber optics and wireless Optical Code-division multiplexing/multiple access systems and provide comprehensive theoretical analysis and simulations for spectral amplitude coding systems operating over realistic environments. The specific objectives of this study are:

- Firstly, the analysis and investigation of PDC in fiber-optic CDMA systems.

- Investigations of new code designs that can support multiclass traffic demands such as the multi-length carrier-hopping prime codes.

- The next objective is to adopt and apply such codes in wireless schemes such as WIR.

- To propose new algorithms suitable for wireless optical domain in order to alleviate the performance floor set by the MAI.

1.4 Major contribution of the thesis

Keeping the aims and objectives in mind during the course of research, the major contributions presented in this thesis are:

- Investigation and analysis of PDC based SAC with physical impairments.

- Signal-to-noise ratio (SNR) criterion is used to propose the optimal value of photodetector gain. In addition, the system performance, with consideration of MAI, shot noise, thermal noise, bulk and surface leakage currents is also evaluated.

- A novel encoding/decoding architecture based on PDC is presented.

- Analytical expressions for BER and SNR derived for PDC with common zero code (CZC).

- A new family of spreading sequences called MCMLCs to support single-rate and multi-rate traffic demands is constructed.

- The proposed sequence is implemented on an efficient encoding and compact decoding devices.

- The bit error rate performance of wireless systems such as WIR is analysed based on PDCs and proposed encoding and decoding structures.

1.5   Thesis Structure

Following this, chapter 2 begins with the quick discussion of the FO-CDMA and WIR systems presented in the literature. It also briefly outlines the working principles of spectral amplitude coding and discusses the properties of perfect difference codes. Chapter 3 presents the analysis of PDC based OCDMA system in terms of bit error rate and signal-to-noise ratio. The analysis takes into account the effects of MAI, shot noise, bulk leakage current, thermal noise, APD gain mismatch and uniformity loss. A major problem in OCDMA system is MAI, in chapter 4 a novel encoder/decoder design is proposed utilizing common zero code technique for optical code division multiplexing system using PDCs as spreading sequences to deal with this problem. The proposed design maintains a constant MAI floor and hence making it simple at the receiver to cancel it. In chapter 5 a family of spreading sequences is constructed based on Manchester-coding, Modified Legendre sequences to be used in OCDM/OCDMA systems suitable for multiclass traffic. In chapter 6, the perfect difference codes for the first time to the best of author's knowledge are applied and their bit error rate performance is analyzed in wireless infrared system. Finally chapter 7 concludes the thesis by outlining the summary and future directions.

1.6   Summary

This chapter provides the overview of optical communication systems. In the second section the author presents the arguments which motivated him to investigate and analyse the performance of optical communication systems based on code-division multiplexing/multiple-access techniques with special focus on perfect difference codes as spreading sequences. Next, the aims and objectives of the work carried under this thesis are listed which are followed by the major contributions of this thesis. Finally the structure of the thesis is laid down.

2. Background & Literature Review

This chapter begins with the background and literature review of optical communication systems focusing on those which are using CDMA as multiple-access techniques. A brief overview of fiber-optic CDMA, wireless infrared systems, spectral-amplitude coding systems, and perfect difference code is given.

2.1 Background

Spread-spectrum CDMA has been extensively studied in the areas of satellite and mobile radio communications. [6-9]. In recent years, the use of CDMA in local area networks has also attracted much interest of researchers [10]. CDMA offers several advantages over conventional multiple-access techniques, such as carrier-sense multiple-access with collision detection (CSMA/CD) and ALOHA [11], in environments with the heavy-load bursty traffic and fast signaling rates. It also permits the users to asynchronously access the same transmission medium with no waiting time.

In general, optical signal processing techniques in optical CDMA can be classified as *incoherent* and *coherent*. In incoherent systems the intensities of

optical pulses are processed, while in coherent systems the fields of optical pulses are processed. In coherent signal processing, the optical pulse in every code sequence generated at an optical encoder are phase coherent and the optical fields of all these coherent pulses are superimposed in an optical decoder. Because of using phase information, a coherent technique allows the use of bipolar (−1, +1) code sequences, and therefore offers a natural discrimination against interference from other codes. Research has shown that the optical encoders and decoders for coherent systems can be made of, for example, diffraction gratings and lenses with phase masks in between [12] or by fiber-optical ladder networks [02, 13-16]. In general, coherent detection gives better performance [17], but is much more difficult to implement, requiring tight control over the phase of the signal and increase the system complexity and sensitivity.

Noncoherent optical CDMA techniques dominate their coherent counterparts due to their ease of practical implementation and include time spreading, frequency hopping, and spatial spreading [18]. In optical systems, which mainly use amplitude modulation, also known as or on-off keying (OOK), with direct detection, the traditional bipolar spreading sequences designed for CDMA won't work because the laser amplitudes cannot be negative. This raises the need of investigating different techniques and codes for spread-spectrum CDMA specially tailored to be used in optical communication systems. Further, such codes must also ensure the less complicated implementation and improved system performance.

The OCDMA has been applied in both wired and wireless mediums. The following sections briefly discuss the applications of spread-spectrum CDMA and related issues in fiber-optics LANs, wireless LANs and Personal Area Networks (PAN).

2.2   Fiber-Optic CDMA

Next generation telecommunication networks are expected to provide a variety of integrated narrowband and broadband bandwidth-hungry services to the customers. Conventional networks using bandwidth-limited media, such as twisted pairs and coaxial cables, will not be able to integrate these broadband services sufficiently. Therefore, the problem of bandwidth limitation needs to be addressed.
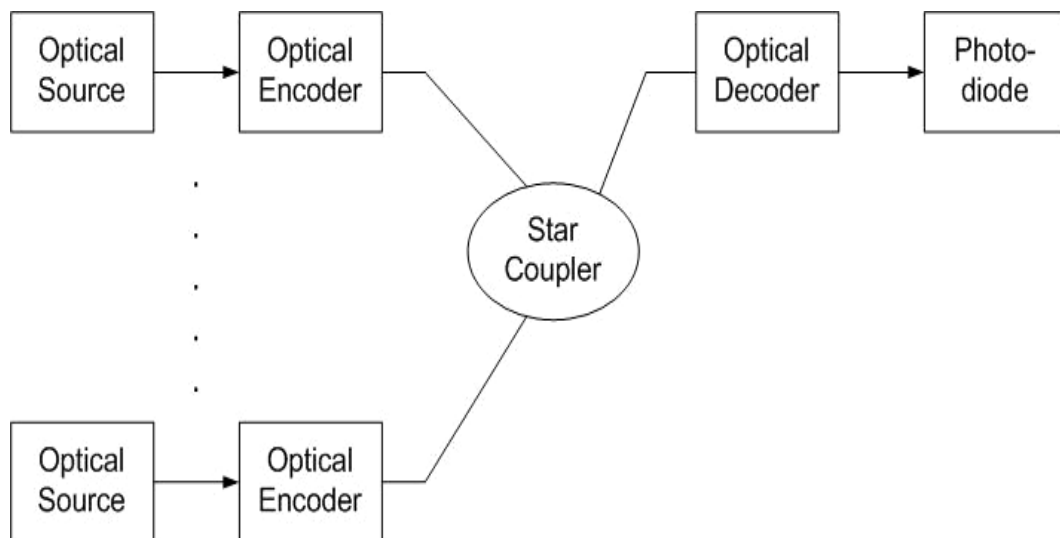
Figure 2-1: Optical CDMA System

The advanced developments in the fiber optics for the past two decades have made possible the use of optical fibers as transmission media in modern communication systems [13, 19] and are proved to be handy when it comes to addressing the issue of bandwidth. The use of optical fibers for such communication links offer several advantages over its counterparts, mainly, huge bandwidth, low signal attenuation, inherent security mechanism, smaller cross sectional area, and cheap cost. As a result, optical fibers have become an integral part of telecommunication systems and networks.

Although most popular electrical local or metropolitan area networks have used a bus or ring topology, most work on optical fiber networks in the past has assumed the use of a passive star topology because of power budget considerations [20]. Figure 2-1 shows a typical FO-CDMA system based on star topology. More

recently, however, the commercial development of optical amplifiers (Erbium Doped Fiber Amplifiers (EDFAs), Semiconductor Optical Amplifiers (SOAs), and Raman amplifiers) has made the fiber bus a feasible proposition [21].

Traditionally, the fiber-optic LANs use either time-division or wavelength-division multiplexing requiring, time or frequency management, respectively. Optical CDMA offers an interesting alternative for LAN because neither time management nor frequency management is required. As the dedicated time or wavelength slots do not have to be allocated so statistical multiplexing gains can be high. Unlike Optical TDMA and WDMA, the maximum transmission capacity is soft-limited, i.e., dependent on the number of active users.

2.2.1 Transmitter and Receiver operation of FO-CDMA Systems

In intensity, OOK system, each user's data encoded optically in an optical encoder that maps each bit into a very high rate optical sequence as shown in Figure 2.2, substantially increasing the bandwidth occupied by the transmitted signal [15, 21- 24]. This, translates into the need of large set of code sequences in order to support many subscribers, which in turn mean that very narrow pulses are required making electronic processing difficult.
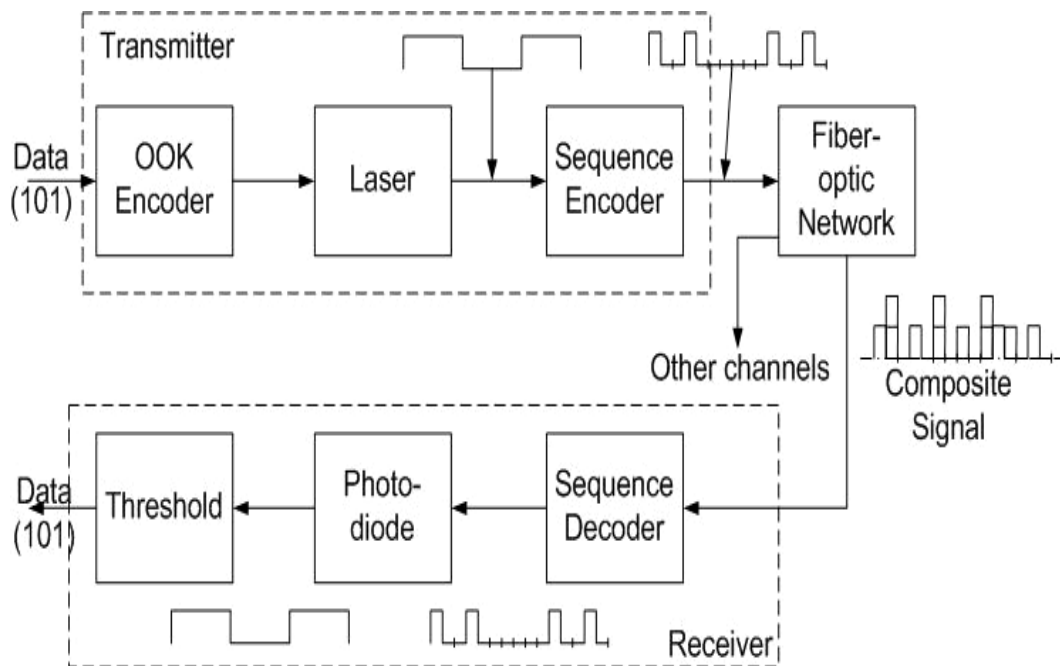
Figure 2-2: Transmitter and receiver model for FO-CDMA system.

In Figure 2.2, a pulse laser source is intensity-modulated by electrical data bits. Next each slot is divided into chips by the sequence encoder where the number of chips in a slot equals to the length of the spreading code consisting of 1 and 0 allocated for users. Then, this spreaded signal is transmitted to the fiber optic network where it is combined positively with the signals of other users generating a composite signal. The same composite signal is received by each user in star broadcast network shown in Figure 2.1. At the receiver, the composite signal is decoded by the copy of desired user's signal spreading sequences which is then photodetected to generate electrical signals. All other received signals other than the desired users are MAI. Finally, a threshold makes the decision of data bit 1 or 0 depending on the intensity of received signal.

2.2.2 LANs versus long-haul optical communication networks

Local area networks (LANs) needs to support multiple users and preferably asynchronously, while wide area networks (WANs) are either point-to-point or multipoint. Therefore, to maintain synchronization in WANs is comparatively easier and most effective technique when compared to LANs. Consequently, dense-wavelength division multiplexing (DWDM) and coarse wavelength-division multiplexing (CWDM) are the preferred methods of data transportation over single mode fibers. Currently, all modern transatlantic cable systems and other long-haul networks are based on DWDM circuits [79].

On the other hand, optical CDMA can perform certain network applications through optical processing, like addressing and routing without resorting to complicated multiplexers or de-multiplexers. Furthermore, it also enables asynchronous mode of data transmission that can simplify network management and control. Therefore, OCDMA is an attractive candidate for LAN applications. Particularly, OCDMA can provide a secure network connection providing dynamic encoding.

The main reasons of DWDM being extensively used in WANs are following [80]:

- Bandwidth multiplication
- Provides extra-resilience
    - Optical circuit protection around ring

- New services

- Improves scalability

- Permits multiple logical topologies over single physical MAN

While the CDMA is well-suited for LANs because of their:

- Asynchronous access

- Selective addressing capability, and

- Low MAI

This thesis therefore focuses its attention on the fiber-optics CDMA based LANs.

2.3   Wireless Infrared (WIR) Systems

Constraints associated with radio wireless network such as, congested and regulated frequency spectrum, limited bandwidth, and interference with other products, etc. have provided the motivation to look at other means of achieving high-speed wireless connectivity for indoor LAN applications. Infrared (IR) is one such alternative, which was first proposed for indoor optical wireless communications in 1979 [25], and is now established as the basis of indoor high-speed communication network. In recent years, the WLAN and Bluetooth technologies have become widespread in the home and office, confirming the demand for such indoor devices.

The notable advantages of IR include:

- it offers potentially huge unregulated bandwidth worldwide and spans wavelengths of 700 – 1500 nm potentially supporting 200 THz of bandwidth [26],

- inherent security as the signal is confined to the room,

- it is capable of supporting high data rates demanded by the multimedia applications.

- no interference with EM spectrum,

- lightweight, low cost and readily available components.

Unfortunately, WIR system has severe drawbacks.

- Ambient light,

- shot noise,

- path loss

- dispersion associated with diffuse infrared systems, and

- multiple access interference (MAI)

The shot noise, path loss and dispersion drives the requirement for high average optical transmit powers which is achieved through power efficient modulation schemes [27, 28]. A detailed survey of efficient modulation technique is given in [29].

There are a number of compensation techniques used to overcome the effect of noise and signal distortion in IR systems; most of these are inherited from the RF

domain, namely; filtering to reduce noise, equalization to overcome distortion and coding for both. Power and bandwidth efficient modulation schemes are also employed as a means of limiting these undesirable effects. However, there are other solutions that are unique to the IR environment, particularly in the form of diversity techniques. Such systems consist of multiple receivers, limited field of view (FOV) receivers, multiple element receivers and multi-beam transmitters to name a few [37]. A possible technique that can increase the received optical power, mitigate the shadowing effect, and reduce multipath dispersion is multibeam transmitter [30-32].

2.3.1 Infrared Link Designs

In the literature [72-75] Infrared links are classified either on the basis of degree of directionality of the transmitter and receiver or whether the link relies upon the existence of an uninterrupted line-of-sight (LOS) path between the transmitter and receiver (see Figure 2.3). The first criterion is commonly known as non-line of sight and second is termed as line-of-sight.
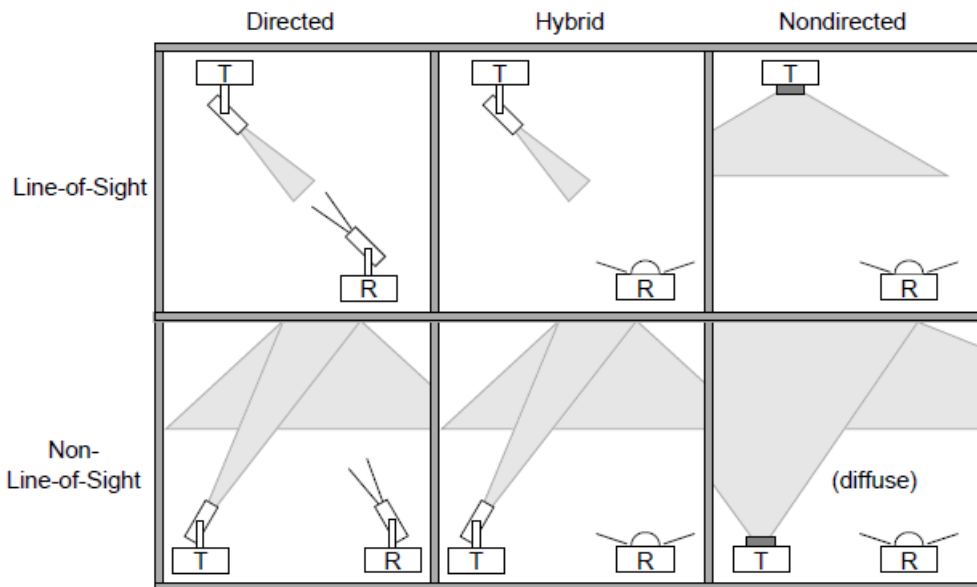
Figure 2-3: Classification of simple Infrared links (Reproduced from [72]).

LOS links rely upon a directed path, while *non-LOS links* generally rely upon reflection of the light from the ceiling or some other diffusely reflecting surface. LOS link design maximizes power efficiency and minimizes multipath distortion. Non-LOS link design increases link robustness and ease of use, allowing the link to operate even when barriers, such as people or cubicle partitions, stand between the transmitter and receiver.

Both these criterion can be further subdivided into three categories as shown in Figure 2.3.

- *Directed links* employ directional transmitters and receivers to establish a link. They improve power efficiency, since they minimize path loss and reception of ambient light noise.

- *Non-directed links* use wide-angle transmitters and receivers, alleviating the need for such pointing. They are particularly useful for mobile terminals.
- *Hybrid links*, combine transmitters and receivers having different degrees of directionality.

The non-directed-non-LOS link design, which is often referred to as a *diffuse link,* achieve greatest robustness and ease of implementation. The advantage of using diffuse channels is the robustness to shadowing or misalignment between the transmitter and the receiver. However, on diffuse channels, optical signals undergo temporal dispersion due to reflections. Therefore, diffuse channels are subject to the multipath distortion that causes ISI.

2.3.2 Intensity modulation/Direct-Detection

Due to the difficulty of making coherent IR receivers, intensity modulation/direct detection (IM/DD) is normally used. In this scheme the instantaneous power of the transmitter is modulated directly and the receiver correspondingly detects the instantaneous power.

Infrared has a similar behavior to that of visible light. It is absorbed by dark objects, diffusely reflected by light-colored objects and directionally reflected from shiny surfaces. IR transmission can penetrate through glass, but is unable to penetrate opaque structures like walls and ceilings which mean that the same optical carrier can be reused in an adjacent room without interference. IR systems do not suffer from the effects of fade as in the RF systems, this being due to the

small wavelengths of IR when compared to the size of the detector. The lack of fade and the positional stability (slow moving or static objects) of the indoor environment mean that the IR channel characteristics remain stable for considerable periods of time. Although multipath fading is mitigated in infrared systems, multipath propagation does lead to dispersion, causing inter-symbol interference in high-speed systems.

2.3.3 Multiple-Access schemes in WIR Systems

As multiple access schemes in infrared wireless systems, TDMA, FDMA, and CDMA have been investigated [33]. CDMA has attracted much attention due to the following advantages. CDMA does not require a tunable laser with accurate control of wavelength and symbol synchronization that are necessary for TDMA and FDMA. Because of these features, spread spectrum CDMA is considered to be a potential candidate for future WIR networks, fulfilling the demands of mutirate multimedia services. Most infrared wireless CDMA systems use ON-OFF keying (OOK) or pulse position modulation (PPM) as a modulation and *m*-sequences or optical orthogonal codes (OOC) as a signature code sequence [34-36].

The performance of an infrared wireless system using direct sequence spread spectrum techniques in multipath channels depends very much on the partial correlation properties of the spreading sequences used. Ideally, a spreading sequence should have zero sidelobes in its periodic and aperiodic auto-correlation functions in order to eliminate multipath dispersion. Unfortunately, no such ideal

sequence exists in the binary field. The penalties incurred in DSSS IR systems are a consequence of non-zero sidelobes of the aperiodic auto-correlation (ACF) and cross-correlation (CCF) functions of the spreading sequences.

To remove these problems three major techniques have been developed. In [35], a sequence inverse keying (SIK) direct sequence spread spectrum modulation technique is proposed to combat the impact of multipath dispersion without the need of any extra circuitry such as equalizers. However, SIK is mainly limited by its spreading factor which reduces the system bandwidth efficiency and its performance in a multipath channel depends very much on the partial correlation properties of the spreading sequences used. To remove the correlation limitations, the complementary SIK (CSIK) is proposed [37]. By transmitting a binary complementary pair (BCP) of sequences and its mate simultaneously, the sidelobes of the aperiodic ACFs and CCFs of the transmitted sequences are summed to near zero at the correlator output, hence eliminating multipath interference almost completely. Though SIK and CSIK are tolerant of interference opening the way of high-data-rate transmission, a key reservation concerning the use of these systems is the spreading factor, which limits system bandwidth efficiency. A method for improving bandwidth and power efficiency is M-ary modulation. A DSSS system using MBOK [38] improves power and bandwidth efficiency while retaining the beneficial properties of DSSS. However, the performance of MBOK depends on the aperiodic correlation functions of the sequences in the set.

2.4 Frequency Domain Coding

There are two types of frequency domain coding employed for CDMA systems: Spectral Amplitude Coding or encoding and the Spectral phase encoding. In a spectral-phase-encoding (SPE) system, different phase shifts at spatially resolved spectral components are obtained by applying a SPE grid [39, 40]. While in a spectral amplitude-encoding (SAE) system, certain frequency or spectral components are transmitted or blocked to transmit a signal [41-44]. The SAE has many advantages when compared to its counterpart SPE. A SAE system is less expensive because it does not require a coherent optical source and relies solely on the presence or absence of pulse power. For the access environment, where cost is one of the most decisive factors, the SAE/OCDM is therefore regarded to be a more promising candidate. The other factor that dominates the use of SAE in optical communication system is the fact that till today controlling the phase of light signals requires much sophisticated and expensive tools then to control the amplitude of light signals.

In frequency-domain-encoding OCDM systems, optical beating interference (OBI) is a major problem. OBI occurs when a photodetector simultaneously receives two or more optical waves with nearly the same wavelength, occurs due to the use of a broadband optical source. It has been shown that the effect of OBI on system performance is critical [45, 46]. As a matter of fact, when the direct-detection scheme is used with either a noncoherent or a coherent source [45-47], the number of users in the SAE/OCDM system is severely decreased by OBI; e.g.,

fewer than 10×1 Gbits/s users can be supported even at a relatively high received optical power of −20 dBm [47]. This makes SAE/OCDM less competitive than WDM, especially in a passive optical network (PON) − based access network environment where link loss up to 30 dB is expected [48]. This problem can be overcome by using a heterodyne detection receiver for a SAE/OCDM system to combat OBI and to improve receiver sensitivity [50]. It is well known that the use of a locally generated optical signal (LO) in the heterodyne receiver could improve the receiver's sensitivity up to 20 dB compared with direct-detection systems [51].

2.4.1 Spectral Amplitude Coding
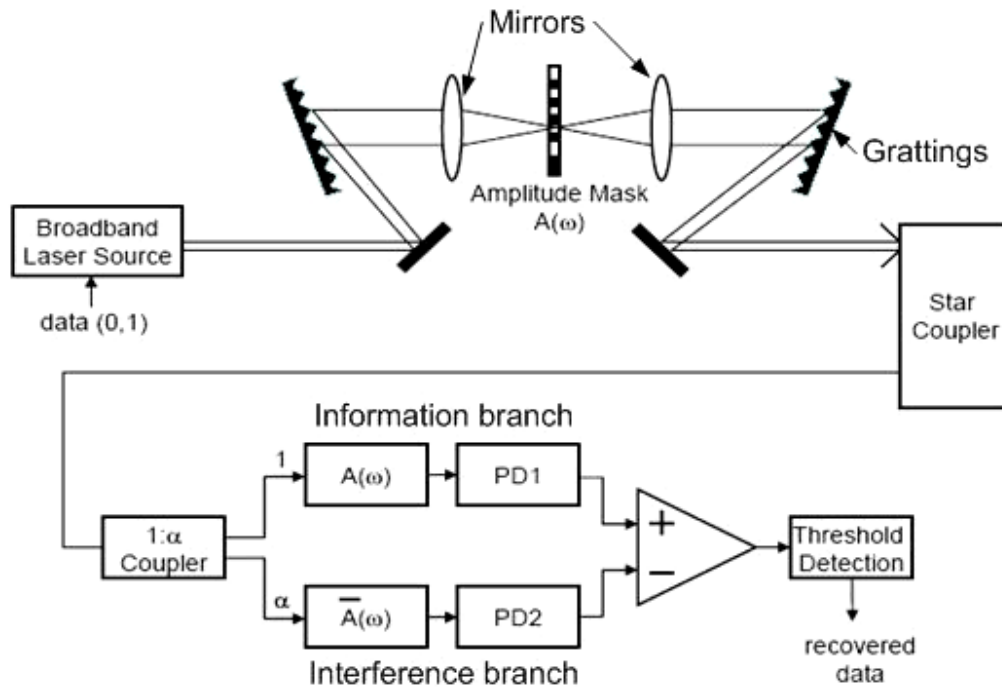
Figure 2-4: Basic Principle diagram of SAE/OCDM system (Reproduced from [50]).

The SAE/OCDM technique was first described by Zaccarin and Kavehrad [42]. Figure 2.4 shows the principle structure of a SAE/OCDM system. At the spectral amplitude encoder, frequency components from a broadband optical source are resolved and encoded by selectively blocking or transmitting certain frequency components in accordance with a signature code. The receiver filters the incoming signal with the same filter (direct decoder to extract information shown by information branch in Figure 2.4) used at the transmitter as well as its complementary filter (complementary decoder to extract interference shown by

interference branch in Figure 2.4). The outputs from these decoders are detected by two photodetectors connected in a balanced fashion. For an interfering signal, depending on the signature code used, a part of its spectral components will match the direct decoder, and the other part will match the complementary decoder. Since the output of the balanced receiver represents the difference between the two photodetector outputs, the interfering channels will be canceled, whereas the matched channel is demodulated; i.e., multiple-access interference (MAI) is canceled in the SAE/OCDM system.

Several signature code sets have been proposed for a SAE/OCDM system, including m-sequence, Hadamard [42, 47], modified quadratic congruence (MQC) code sets [52], and perfect difference codes [4, 5]. Each of these signature code sets can be represented by its length, weight, and in-phase cross correlation (v, w, γ). In the m-sequence code set, $w = v+1/2$ and $\gamma = v+1/4$; the weight and in-phase cross correlation of the Hadamard code set are $v/2$ and $v/4$, respectively. In MQC code, $\gamma = 1$, and for an odd prime p, we have code length $v = p^2 + p$ and weight $w = p+1$. Constructions of these codes can be found in [42, 47, 52]. For PDC, $v = w^2 - w+1$, weight $w = p+1$, where p is a prime number, and $\gamma = 1$.

2.4.2 Mathematical Model of Spectral Amplitude Coding

Let $c_d = [c_d(0), c_d(1), ..., c_d(n-1)]$ and $c_k = [c_k(0), c_k(1), ..., c_k(n-1)]$ be two (0,1) signature codes, then the correlation properties are given by

$$\Phi_{c_d, c_k} = \sum_{i=0}^{v-1} c_d(i) c_k(i) = \begin{cases} w & \text{if } d = k \\ \gamma & \text{if } d \neq k \end{cases} \qquad (2.1)$$

The correlation between $\overline{c_d}$ (a complementary of c_d) and c_k is

$$\Phi_{\overline{c_d}, c_k} = \sum_{i=0}^{v-1} \overline{c_d}(i) c_k(i) = w - \Phi_{c_d, c_k} = \begin{cases} 0 & \text{if } d = k \\ w - \gamma & \text{if } d \neq k \end{cases} \qquad (2.2)$$

In order to cancel the MAI completely, it is necessary to set a ratio between the optical powers that arrive at the two photodetectors $\alpha = \gamma / w - \gamma$ [42, 52]. The cancellation of the interfering signal (when $k \neq d$) by the balanced receiver thus can be seen as

$$\left(\Phi_{c_d, c_k}\right) - \alpha\left(\Phi_{\overline{c_d}, c_k}\right) = \gamma - \frac{\gamma}{w - \gamma}(w - \gamma) = 0 \qquad (2.3)$$

Results from previous research show that a low-weight code, e.g., MQC, is preferable to a high-weight code when OBI is considered, especially when the received optical power is high. In fact, a lower code weight results in a lower signal-to-noise ratio (SNR) if OBI is negligible. This happens in the MQC coded system when the received optical power is low because this optical power is

further reduced by a ratio of α in one of the branches. However, when the received optical power is increased, OBI is increased and becomes ineligible. In this case, compared to an *m*-sequence or Hadamard coded system, a MQC coded system has a higher SNR (i.e., better performance) thanks to its low in-phase cross correlation, i.e., resulting in lower OBI [52].

Next section briefly discuss the one of the spreading sequences utilized in unipolar OCDMA system based on SAC, namely, perfect difference codes.

2.5   Perfect Difference Codes

Perfect difference codes are the special type of cyclic difference set with $(v, w, \gamma = 1)$. The detailed information about the perfect difference codes can be found in [4], [81], and [82]. For the purpose of this thesis we are interested in the following two properties of PDCs:

1. The cross correlation between the two PDCs is unity. This property is exploited to design the decoder to efficiently recover data by suppressing MAI effect.

2. Perfect difference codes are cyclic shifted. The cyclic nature of PDCs is combined with the cyclic nature of Arrayed-waveguide multiplexers to construct compact efficient encoders.

From the property of cyclic difference sets, let $c_k(i)$ denote the ith element of the kth PDC code. The code properties can be written as:

$$\sum_{i=1}^{v} c_k(i)c_l(i) = \begin{cases} w, & k = l \\ 1, & k \neq l \end{cases} \qquad (2.4)$$

The example of Perfect difference Codes for $w=3$ and $v=7$ are shown in Table 2.1.

Table 2-1: Example of Perfect Difference Code.

Perfect difference set for $w=3$ and $v=7$						
1	1	0	1	0	0	0
0	1	1	0	1	0	0
0	0	1	1	0	1	0
0	1	0	1	1	0	1
1	0	1	0	1	1	0
0	1	0	1	0	1	1
1	0	1	0	1	0	1

2.6   Summary

This chapter presents a brief introduction and discusses the related issues to fiber-optic CDMA based local area networks, wireless infrared systems and spectral amplitude coding systems. From the literature review the author envisaged that the optical CDMA can play a key role in the development of high-capacity and high-data rate multimedia supportive communication networks for both wired and wireless mediums. Finally, the last section briefly outlines the properties of

Perfect difference codes particularly suitable for the efficient implementation of encoders and decoders in SAC based OCDMA systems.

In the next chapter, the performance of spectral amplitude coding system based on perfect difference codes described in this chapter is analyzed considering the mismatch losses in the photodetectors of receiver and splitting losses of the multiplexers and de-multiplexers.

3. Performance Analysis of Spectral Amplitude Coding based OCDMA System

In this chapter, the performance of spectral-amplitude coding based OCDMA system is analyzed using Gaussian approximations in terms of bit error rate taking into account, multiple access interference, thermal noise, bulk leakage current, surface leakage current and APD mismatch losses at the detector and splitting losses of the multiplexers/de-multiplexers.

3.1 Introduction

The ever hungry consumers of current and potential future access networks are making Optical Code-Division Multiple-Access (OCDMA) systems more and more attractive in the field of all optical communications as it promises to enable the end users to access the network asynchronously and simultaneously with high level of transmission security [1, 3-5, 53-55]. Designing an OCDMA system, however, imposes a challenge to minimize the influence of multiple-access interference (MAI). Spectral amplitude coding (SAC) techniques are widely been considered to address this issue as the MAI can be theoretically cancelled when

code sequences with fixed in-phase cross-correlation (such as perfect difference codes or Hadamard code) are used [5].

In the most research on OCDMA systems based on PDCs [4, 5], the evaluation of error probability is based on the ideal assumptions such as the gains of APDs used in information extracting and MAI cancelling branches of optical code-division multiple-access (OCDMA) systems receiver are matched or the multiplexers used at transmitter and receiver uniformly splits the input and received power. Such approximations in practice may be an overestimate or underestimate of the actual probability of error. In this chapter, the impact of APD mismatch is analyzed [4, 5] and splitter's uniformity loss [5] in the OCDMA systems based on the perfect difference codes (PDC). The SNR criterion is also used to propose the optimal value of APD gain. In addition, the system performance, with consideration of shot noise, thermal noise, avalanche photodiode (APD), bulk and surface leakage currents, and APD gain mismatch is also evaluated.

The remainder of this chapter is organized as follows. In section 3.2, the structure of the transmitter and receiver is described. Section 3.3 presents the analysis of impairments such as splitter loss and APD mismatch gain. Finally, section 3.4 discusses the experiments and numerical results obtained for the BER and system capacity.

3.2 System Model

In [5], an asynchronous OCDMA system is proposed based on PDCs as shown in Figure 3.1. The analysis is carried out in ideal conditions and is based on some serious assumptions such as the gain of APDs used in receiver of proposed systems are perfectly matched and that the power is splitted uniformly in the splitters used at transmitter and receiver side. In what follows the system proposed in [5] is analyzed considering practical environment and attempt to critically analyze the obtained results and also propose some ways to minimize or overcome the losses.
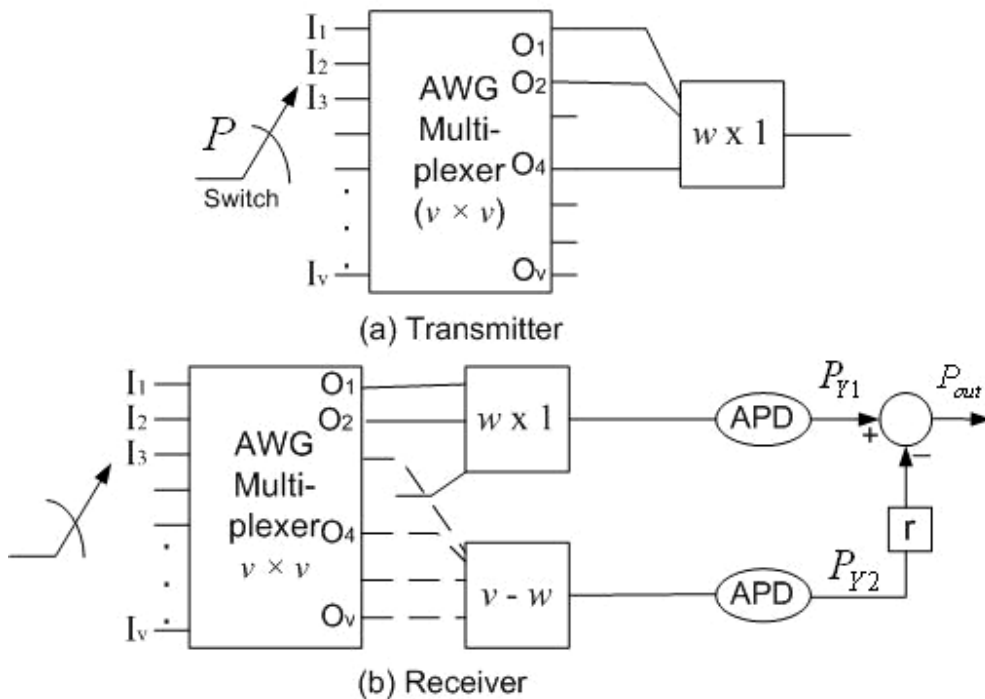
Figure 3-1: SAC-OCDMA system based on perfect difference codes [5].

Each subscriber is assigned a unique code. Each active user transmits a signature sequence of w laser pulses (representing the destination address), over a time frame if mark "1" is transmitted. However, if the data bit is space "0," no pulses are transmitted during the time frame. The system presented in [5] proposes the use of PDC to overcome the limitation of codeword synchronization and power loss incurred in the Spectral Amplitude Coding (SAC)-OCDMA Systems.

3.2.1 Transmitter

The arrayed waveguide grating $v \times v$ wavelength multiplexer (AWG MUX) proposed in [55] is used as encoder and decoder since both it and PDC have a cyclic-shifted property. It is assumed that a broadband optical pulse entering one of the input ports of the AWG MUX is split into a v number of spectral components. Each spectral component follows a unique route through the AWG MUX in accordance with its particular wavelength.

The transmitter shown in Figure 3.1 comprises a switch, a $v \times v$ AWG MUX and a $w \times 1$ coupler. In accordance with the employed PDC, w output ports are selected in advance. When data bit '1' is to be transmitted, a broadband optical pulse is sent to one of the v input ports of the multiplexer. The choice of input port is determined by the switch in accordance with the signature sequence of the destined user. The optical broadband pulse entering the multiplexer is split into v spectral components. These components exit the multiplexer through the w

predetermined output ports and are then combined into a single pulse by the $w \times 1$ coupler and transmitted to the destined user. To transmit bit '1' to a different user, the transmitter uses the switch in front of the AWG MUX to change the input port of the broadband optical pulse in accordance with the codeword sequence of the new user. Consequently, a different group of spectral components exits from the w predetermined output ports. When a '0' data bit is to be transmitted, nothing is actually sent. In this study, it is assumed that l_1, l_2,...,l_w are the spectral components which make up the signature sequence of the destined user.

3.2.2 Receiver

The front of the receiver is implemented by adding a $(v - w) \times 1$ coupler to the transmitter structure. In accordance with the code of the destined user, the received optical pulse is directed to the corresponding input port by the switch in front of the AWG MUX. As described above, the optical pulse is then split into several spectral components and each component follows its own particular route through the AWG MUX. The spectral components, l_1, l_2,...,l_w, exiting from the w predetermined output ports, are collected by the $w \times 1$ coupler and combined into a single optical pulse. This pulse is transmitted to an APD, which responds by outputting the corresponding photoelectron count, Y_1. Meanwhile, the $(v - w) \times 1$ coupler collects the spectral components which exit through all of the output ports of the AWG MUX other than the w predetermined ports. The output of the $(v - w) \times 1$ coupler, referred to as the filtered multiple-access interference (MAI), is

photodetected by a second APD, which outputs the photoelectron count, Y_2. The filtered MAI signal is employed to remove the MAI from the spectral components coupled by the $w \times 1$ coupler, i.e. the residual MAI.

3.3 Performance Analysis

The number of active users is assumed to be N and that there are I interfering users. Furthermore, without loss of generality, it is assumed that the first user is the desired user and that b_0 is the desired bit. The average photon arrival rate λ per pulse at the input of the optical correlator in the first branch is given by.

$$\lambda = \eta P / hf \tag{3.1}$$

where, P is the input power, h is the Planck's constant, f is the optical frequency and η is the APD quantum efficiency. The power of each spectral component is:

$$\lambda = \eta P / vhf \tag{3.2}$$

Each user contributes one spectral component in the desired user's signal; therefore, the total interference due to MAI is given by:

$$I = \sum_{k=1}^{K} i_k \tag{3.3}$$

3.3.1 APD Mismatch Analysis

Referring to the receiver shown in Figure 3.1, in the existing systems proposed in literature, the analysis is based on the assumptions that the two photodetectors at

information and interference branches are completely matched. This, however, may not be the case in practice. To investigate this, this section considers the effects of photodetector gain mismatches on the system's bit error rate performance. This work is published in [83].

Given $N = I$ and the desired bit $b_0 = 1$, the mean and variance of output Y_1 after the sampler in the first branch can be expressed as:

$$\mu_{y1} = G_1 T_c \left[(w + I)\lambda + \frac{I_{b1}}{e} \right] + \frac{T_c I_{s1}}{e} \tag{3.4}$$

$$\sigma_{y1}^2 = G_1^2 F_{e1} T_c \left[(w + I)\lambda + \frac{I_{b1}}{e} \right] + \frac{T_c I_{s1}}{e} + \sigma_{th}^2 \tag{3.5}$$

where, G_1 is the average APD gain of upper APD, the subscript 1 denotes the parameter for branch 1, T_c is the chip duration, I_b is the bulk leakage current, I_s is the surface leakage current, e is the electron charge, F_e is the excess noise factor given as:

$$F_e = k_{eff} G + (2 - 1/G)(1 - k_{eff}) \tag{3.6}$$

here k_{eff} is the APD effective ionization ratio and, σ_{th}^2 is the variance of thermal noise given as:

$$\sigma_{th}^2 = \frac{2 K_b T_n T_c}{e^2 R_L} \tag{3.7}$$

where K_b is the Boltzman's constant, T_n is the receiver noise temperature, and R_L is the receiver load resistance.

Similarly, given I and $b_0 = 0$, the mean and variance of Y_1 is given by (3.8) and (3.9), respectively.

$$\mu'_{y1} = G_1 T_c \left[I\lambda + \frac{I_{b1}}{e} \right] + \frac{T_c I_{s1}}{e} \qquad (3.8)$$

$$\sigma^{2'}_{y1} = G_1^2 F_{e1} T_c \left[I\lambda + \frac{I_{b1}}{e} \right] + \frac{T_c I_{s1}}{e} + \sigma^2_{th} \qquad (3.9)$$

Given I, the mean and variance of the output Y_2 can be expressed by (3.10) and (3.11), respectively.

$$\mu_{y2} = G_2 T_c \left[(w-1)I\lambda + \frac{I_{b2}}{e} \right] + \frac{T_c I_{s2}}{e} \qquad (3.10)$$

$$\sigma^2_{y1} = G_2^2 F_{e2} T_c \left[(w-1)I\lambda + \frac{I_{b2}}{e} \right] + \frac{T_c I_{s2}}{e} + \sigma^2_{th} \qquad (3.11)$$

where, G_2 is the average APD gain of lower APD and the other parameters are same as described above, the subscript 2 denotes the parameter for branch 2. After subtracting $Y_2 r$ from Y_1, the mean of Y is obtained as given by (3.12) for $b_0 = 1$ and $b_0 = 0$, respectively.

$$E(Y) = \begin{cases} \mu_Y = G_1 T_c \left[\begin{array}{c} (w+I)\lambda - \\ r\dfrac{G_2}{G_1}(w-1)I\lambda \end{array} \right] + \dfrac{T_c G_1}{e} \left[I_{b1} - rI_{b2}\dfrac{G_2}{G_1} \right] \\ + \dfrac{T_c G_1}{e} \left[I_{s1} - rI_{s2}\dfrac{G_2}{G_1} \right] \\ \mu_Y^{'} = G_1 T_c \left[\begin{array}{c} I\lambda - \\ r\dfrac{G_2}{G_1}(w-1)I\lambda \end{array} \right] + \dfrac{T_c G_1}{e} \left[I_{b1} - rI_{b2}\dfrac{G_2}{G_1} \right] \\ + \dfrac{T_c G_1}{e} \left[I_{s1} - rI_{s2}\dfrac{G_2}{G_1} \right] \end{cases} \qquad (3.12)$$

The mean for data bit 1 and 0 given in Equation (3.12) are used to calculate the probability of error using Gaussian approximations.

3.3.2 Combined APD Mismatch and Splitter loss Analysis

Referring to the transmitter and receiver shown in Figure 3.1, in the existing systems proposed in literature, the analysis is based on the assumptions that the power at the AWG multiplexers is splitted uniformly. This, however, may not be the case in practice. To investigate this, this section considers the effects of splitting mismatch losses combined with photodetector gain mismatches on the system's bit error rate performance.

For K transmitter/receiver pairs, the optical signal of the k-th user can be written as:

$$S_k(t) = b_k P \sum_{l=0}^{v-1} \alpha_{l,k} c_{l,k} \delta(t - l\tau_c) \qquad 0 \leq t \leq v, b_k \in \{0,1\}, c_{l,k} \in \{0,1\} \quad (3.13)$$

Where P is a user's received power, b_k is the k-th user's binary data bit (0, 1), $c_{l,k}$ is the signature code waveform generated by the PDC sequence assigned to the kth user, $\delta(t)$ is the unit-rectangular pulse of duration τ_c, v is the sequence length, and l is the output port of the splitter at transmitter. It can also be found that the $\alpha_{l,k}$ is a random variable whose value varies from $\dfrac{P}{v} - \dfrac{ls}{2}$ to $\dfrac{P}{v} + \dfrac{ls}{2}$.

Where ls is the uniformity loss of the splitter in dB.

This is then inputted to the star coupler which accumulates the resultant powers of each user's coupler. Hence, the signal at the star coupler will be:

$$S_{star}(t) = \sum_{k=1}^{K} b_k P \sum_{l=0}^{v-1} \alpha_{l,k} c_{l,k} \delta(t - l\tau_c) \qquad (3.14)$$

It is assumed that, the received power P_r is equal to the input power P, which again will be splitted into v components by second splitter at the receiver. The received signal for user 1 can be modeled as:

$$S_r(t) = \sum_{m=0}^{v-1} \sum_{k=1}^{K} b_k P \sum_{l=0}^{v-1} \alpha_{l,k} c_{l,k} \delta(t - l\tau_c) . \beta_{m,1} c_{m,1} \delta(t - m\tau_c) \qquad (3.15)$$

$$S_r(t) = P\sum_{k=10}^{K} b_k \sum_{m=0}^{v-1} \sum_{w=0}^{v-1} \alpha_{l,k}\beta_{m,1}c_{l,k}c_{m,1}\delta(t-l\tau_c)\delta(t-m\tau_c) \qquad (3.16)$$

where m denotes the output ports of the splitter at receiver, and $\beta_{m,k}$ is same as $\alpha_{w,k}$ but at the receiver side, $c_{m,1}$ is the copy of spreading code for user 1 at receiver side. This signal is inputted to the coupler at the receiver and it can be divided into the wanted component and unwanted component as:

$$
\begin{aligned}
S_r(t) = & Pb_1\sum_{m=0}^{v-1}\sum_{l=0}^{v-1} \alpha_{l,1}\beta_{m,1}c_{l,1}c_{m,1}\delta(t-l\tau_c)\delta(t-m\tau_c) + \\
& P\sum_{k=2}^{K} b_k \sum_{m=0}^{v-1}\sum_{w=0}^{v-1} \alpha_{l,k}\beta_{m,1}c_{l,k}c_{m,1}\delta(t-l\tau_c)\delta(t-m\tau_c)
\end{aligned}
\qquad (3.17)
$$

The first term in above equation denotes the wanted signal. This will only be achieved when all the spectral components that exited from the AWG multiplexer at the transmitter side are the same as that which exit from the receiver. The second term in the above equation represents the unwanted component in the desired signal; this is achieved when the spectral components exited from the AWG multiplexer at the transmitter side do not match with those that exited at the receiver side.

For K system users and given I interfering users and data bit $b_k = 1$; the mean and variance of output Y_1 can be expressed as:

$$\mu_{Y_1} = G_1 T_c \left[\begin{array}{l} P b_1 \sum\limits_{m=0}^{w}\sum\limits_{l=0}^{w} \alpha_{l,1}\beta_{m,1}c_{l,1}c_{m,1}\delta(t-l\tau_c)\delta(t-m\tau_c) + \\[2mm] P\sum\limits_{k=2}^{K} b_k \sum\limits_{m=0}^{w}\sum\limits_{l=0}^{w} \alpha_{l,k}\beta_{m,1}c_{l,k}c_{m,1}\delta(t-l\tau_c)\delta(t-m\tau_c) \\[2mm] + \dfrac{I_{b1}}{e} \end{array} \right] + \dfrac{T_c I_{s1}}{e} \qquad (3.18)$$

$$\sigma_{Y_1}^{\;2} = G_1^2 F e_1 T_c \left[\begin{array}{l} P b_1 \sum\limits_{m=0}^{w}\sum\limits_{l=0}^{w} \alpha_{l,1}\beta_{m,1}c_{l,1}c_{m,1}\delta(t-l\tau_c)\delta(t-m\tau_c) + \\[2mm] P\sum\limits_{k=2}^{K} b_k \sum\limits_{m=0}^{w}\sum\limits_{l=0}^{w} \alpha_{l,k}\beta_{m,1}c_{l,k}c_{m,1}\delta(t-l\tau_c)\delta(t-m\tau_c) \\[2mm] + \dfrac{I_{b1}}{e} \end{array} \right]$$
$$+ \dfrac{T_c I_{s1}}{e} + \sigma_{th}^2 \qquad (3.19)$$

where, G_1 is the average APD gain of upper APD, e is the electron charge, I_b is the APD bulk leakage current, I_s is the APD surface leakage current, and T_c is the chip duration, F_e is the excess noise factor, and σ_{th} is the variance of thermal noise (the subscript 1 represent the terms of upper branch).

Similarly, given I and $b_k = 0$

$$\mu'_{Y_1} = G_1 T_c \left[\begin{array}{l} P\sum\limits_{k=2}^{K} b_k \sum\limits_{m=0}^{w}\sum\limits_{l=0}^{w} \alpha_{w,k}\beta_{m,1}c_{l,k}c_{m,1}\delta(t-l\tau_c)\delta(t-m\tau_c) \\[2mm] + \dfrac{I_{b1}}{e} \end{array} \right] + \dfrac{T_c I_{s1}}{e} \qquad (3.20)$$

$$\sigma_{Y_1}^{2'} = G_1^2 F e T_c \left[\begin{array}{c} P\sum_{k=2}^{K} b_k \sum_{m=0}^{w}\sum_{l=0}^{w} \alpha_{l,k}\beta_{m,1}c_{l,k}c_{m,1}\delta(t-l\tau_c)\delta(t-m\tau_c) \\ +\dfrac{I_{b1}}{e} \end{array} \right] + \dfrac{T_c I_{s1}}{e} + \sigma_{th}^2 \qquad (3.21)$$

and Y_2 can be expressed similarly as Y_1. Given I:

$$\mu_{Y_2} = G_2 T_c \left[\begin{array}{c} P\sum_{k=2}^{K} b_k \sum_{m=0}^{v-w}\sum_{w=0}^{v-w} \alpha_{w,k}\beta_{m,1}c_{w,k}c_{m,1}\delta(\lambda-w\lambda_c)\delta(\lambda-m\lambda_c) \\ +\dfrac{I_{b2}}{e} \end{array} \right] + \dfrac{T_c I_{s2}}{e} \qquad (3.22)$$

$$\sigma_{Y_2}^2 = G_2^2 F e_2 T_c \left[\begin{array}{c} P\sum_{k=2}^{K} b_k \sum_{m=0}^{v-L}\sum_{w=0}^{v-L} \alpha_{w,k}\beta_{m,1}c_{w,k}c_{m,1}\delta(\lambda-w\lambda_c)\delta(\lambda-m\lambda_c) \\ +\dfrac{I_{b2}}{e} \end{array} \right]$$
$$+ \dfrac{T_c I_{s2}}{e} + \sigma_{th}^2 \qquad (3.23)$$

where, G_2 is the average APD gain of lower APD, (the subscript 2 represent the terms of lower branch).

For the nominal case, that is $G_1 = G_2 = G$, the MAI is cancelled for the condition shown in (3.24).

$$r = 1/(w-1) \qquad (3.24)$$

After subtracting the signal rY_2 from Y_1, the mean and variance of output Y can be expressed as:

$$\mu_Y = G_1 T_c P.$$

$$
\begin{bmatrix}
b_1 \displaystyle\sum_{m=0}^{w}\sum_{l=0}^{w} \alpha_{l,1}\beta_{m,1}c_{l,1}c_{m,1}\delta(t-l\tau_c)\delta(t-m\tau_c) + \\[2mm]
\displaystyle\sum_{k=2}^{K} b_k \sum_{m=0}^{w}\sum_{w=0}^{w} \alpha_{l,k}\beta_{m,1}c_{l,k}c_{m,1}\delta(t-l\tau_c)\delta(t-m\tau_c) - \\[2mm]
r\dfrac{G_2}{G_1}\left(\displaystyle\sum_{k=2}^{K} b_k \sum_{m=0}^{v-w}\sum_{l=0}^{v-w} \alpha_{l,k}\beta_{m,1}c_{l,k}c_{m,1}\delta(t-l\tau_c)\delta(t-m\tau_c) \right)
\end{bmatrix} +
\tag{3.25}
$$

$$\frac{G_1 T_c}{e}\left(I_{b1} - \frac{G_2 r I_{b2}}{G_1} \right) + \frac{T_c}{e}\left(I_{s1} - r I_{s2} \right)$$

$$\mu_Y' = G_1 T_c P.$$

$$
\begin{bmatrix}
\displaystyle\sum_{k=2}^{K} b_k \sum_{m=0}^{w}\sum_{l=0}^{w} \alpha_{l,k}\beta_{m,1}c_{l,k}c_{m,1}\delta(t-l\tau_c)\delta(t-m\tau_c) - \\[2mm]
r\dfrac{G_2}{G_1}\left(\displaystyle\sum_{k=2}^{K} b_k \sum_{m=0}^{v-w}\sum_{l=0}^{v-w} \alpha_{l,k}\beta_{m,1}c_{l,k}c_{m,1}\delta(t-l\tau_c)\delta(t-m\tau_c) \right)
\end{bmatrix}
\tag{3.26}
$$

$$+ \frac{G_1 T_c}{e}\left(I_{b1} - \frac{G_2 r I_{b2}}{G_1} \right) + \frac{T_c}{e}\left(I_{s1} - r I_{s2} \right)$$

Then variances of Y are given by equations (3.27).

$$
Var(Y) = \begin{cases}
\sigma_Y^2 = \sigma_{y1}^2 + r^2 \sigma_{y2}^2 \\
\sigma_Y^{2'} = \sigma_{y1}^{2'} + r^2 \sigma_{y2}^2
\end{cases}
\tag{3.27}
$$

The threshold detector uses the statistic Y to identify the received data bit in accordance with a decision threshold. If the received photoelectron count, Y, is greater than the threshold, bit '1' is declared, alternatively, bit '0'. The threshold is specified according to three different decision rules presented in [5]:

Rule 1:

$$\theta = \frac{1}{2}\left(\mu_Y + \mu_Y'\right) \tag{3.28}$$

Rule 2:

$$\theta = \frac{\sigma_Y' \mu_Y + \sigma_Y \mu_Y'}{\sigma_Y + \sigma_Y'} \tag{3.29}$$

Rule 3:

$$\theta = \frac{\overline{\sigma_Y'} \mu_Y + \overline{\sigma_Y} \mu_Y'}{\overline{\sigma_Y} + \overline{\sigma_Y'}} \tag{3.30}$$

$$\sigma_Y^2 = \sigma_{y1}^2 + r^2 \sigma_{y2}^2 \tag{3.31}$$

$$\sigma_Y^{2'} = \sigma_{y1}^{2'} + r^2 \sigma_{y2}^2 \tag{3.32}$$

where:

$$\left(\overline{\sigma_{y1}}\right)^2 = G_1^2 F_{e1} T_c \left[\left(w + \overline{I}\right)\lambda + \frac{I_{b1}}{e}\right] + \frac{T_c I_{s1}}{e} + \sigma_{th}^2 \tag{3.33}$$

$$\left(\overline{\sigma_{y1}'}\right)^2 = G_1^2 F_{e1} T_c \left[\overline{I}\lambda + \frac{I_{b1}}{e}\right] + \frac{T_c I_{s1}}{e} + \sigma_{th}^2 \tag{3.34}$$

$$\left(\overline{\sigma_{y2}}\right)^2 = G_2^2 F_{e2} T_c \left[(w-1)\overline{I}\lambda + \frac{I_{b2}}{e}\right] + \frac{T_c I_{s2}}{e} + \sigma_{th}^2 \tag{3.35}$$

and $\overline{I}$ can be expressed as:

45

$$\bar{I} = \sum_{i=1}^{N-1} i \times \binom{N-1}{i}\left(\frac{1}{2}\right)^{N-1} \tag{3.36}$$

The bit error can be derived from (3.37) to (3.41):

$$
\begin{aligned}
Pe(error \mid N = n) &= Pe(Y \geq \theta \mid N = n, b_o = 0) \times Pe(b_o = 0) \\
&+ Pe(Y < \theta \mid N = n, b_o = 1) \times Pe(b_o = 1)
\end{aligned}
$$

$$
\begin{aligned}
&= \frac{1}{2}\sum_{i=o}^{n-1} Pe(Y \geq \theta \mid I = i, b_o = 0) \times Pe(I = i \mid N = n, b_o = 0) \\
&+ \frac{1}{2}\sum_{i=o}^{n-1} Pe(Y < \theta \mid I = i, b_o = 1) \times Pe(I = i \mid N = n, b_o = 1)
\end{aligned} \tag{3.37}
$$

where

$$
\begin{aligned}
Pe(Y \geq \theta \mid I = i, b_o = 0) &= \int_{\theta}^{\infty} \frac{1}{\sqrt{2\pi\sigma_{Y0}^2}} \exp\left[-\frac{(y - \mu_{Y0})^2}{2\sigma_{Y0}^2}\right] dy \\
&= \frac{1}{2}erfc\left(\frac{\theta - \mu_{Y0}}{\sqrt{2\sigma_{Y0}^2}}\right)
\end{aligned} \tag{3.38}
$$

$$
\begin{aligned}
Pe(Y < \theta \mid I = i, b_o = 1) &= \int_{-\infty}^{\theta} \frac{1}{\sqrt{2\pi\sigma_{Y1}^2}} \exp\left[-\frac{(y - \mu_{Y1})^2}{2\sigma_{Y1}^2}\right] dy \\
&= \frac{1}{2}erfc\left(\frac{\mu_{Y1} - \theta}{\sqrt{2\sigma_{Y1}^2}}\right)
\end{aligned} \tag{3.39}
$$

$$
\begin{aligned}
Pe(I = i \mid N = n, b_o = 0) &= \Pr(I = i \mid N = n, b_o = 1) \\
&= \binom{n-1}{i}\left(\frac{1}{2}\right)^{n-1}
\end{aligned} \tag{3.40}
$$

and, $erfc(\cdot)$ stands for the complementary error function, as defined in (3.30)

$$erfc\,(x) = \frac{2}{\sqrt{\pi}} \int_{x}^{\infty} \exp\left(-y^2\right) dy \qquad (3.41)$$

The signal-to-noise ration then can be calculated as:

$$SNR\ = \frac{\left(\mu_Y' - \mu_Y\right)^2}{\left(\sigma_Y^2 + \sigma_Y^{2'}\right)} \qquad (3.42)$$

3.4   Experiments & Results

Figure 3.2 shows the bit error rate versus number of simultaneous users for three rules of selecting the threshold. For our experiments, the gain of the upper branch's APD, which is used to extract the information of the desired user, is kept fixed and set to the typical value of 100 [4, 5]. The gain of the lower branch's APD is incremented or decremented in steps of 5%. The power received per pulse for most plot is assumed to be fixed at $P_r = w \times 10 \mu W$. The values of shot noise, thermal noise, and bulk and surface leakage currents, are taken separately for both the APDs. We use the value of r obtained from Equation (3.24) which assume that the gains of both APDs are perfectly matched. However, in practice this is not the case. As a result, the MAI is not completely cancelled, and consequently only a 5% difference between the gains of the two APDs causes more than 50% reduction in the system capacity, as shown in Figure 3.2. This problem can be compensated, if the gains of the two APDs used are accurately measured under

the prevailing conditions. This condition for the complete cancellation of MAI is defined by $r = G_1/G_2(w - 1)$.
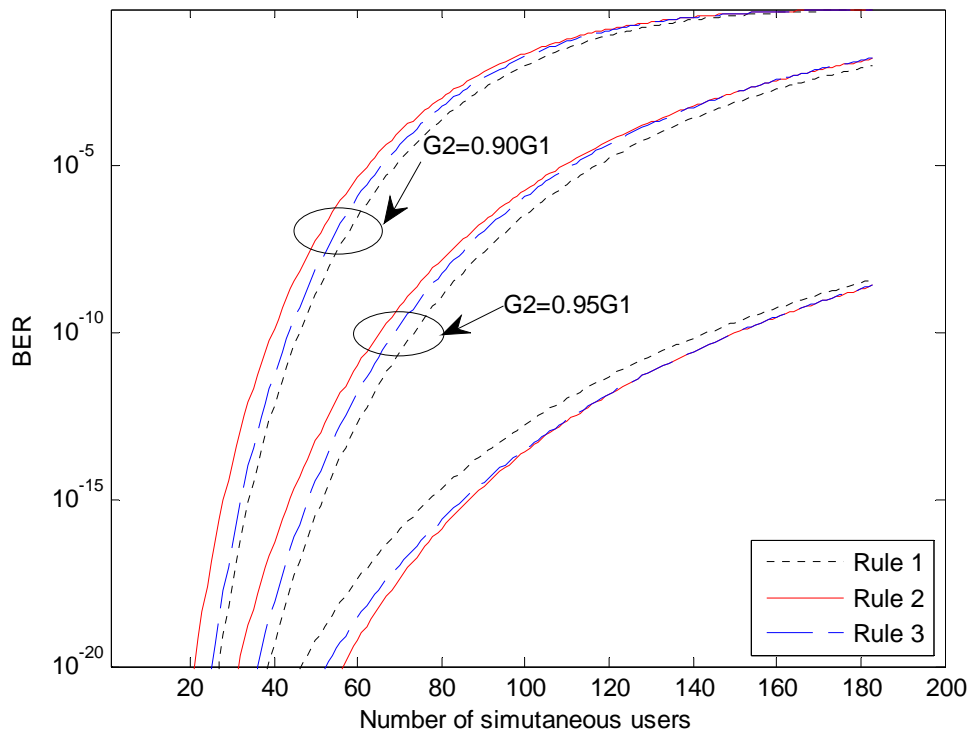
Figure 3-2: BER probability for l = 14 and splitter loss of 0.5 dB.

Fig. 3.3 plots the SNR versus the Average APD gain with variable F_e on a log-log scale for different power levels. The plot illustrates that in cases when received power is lower there is an optimal value of APD gain as can be seen in the case of – 58.5 dB of power. In this case the optimal value is around 10. For fixed value of F_e say 2 shown by dotted lines for respective power levels, we obtain a linear increase in the SNR up to some optimal value of gain and then it saturates

afterwards. A high value of APD gain beyond 100 degrades the SNR performance.
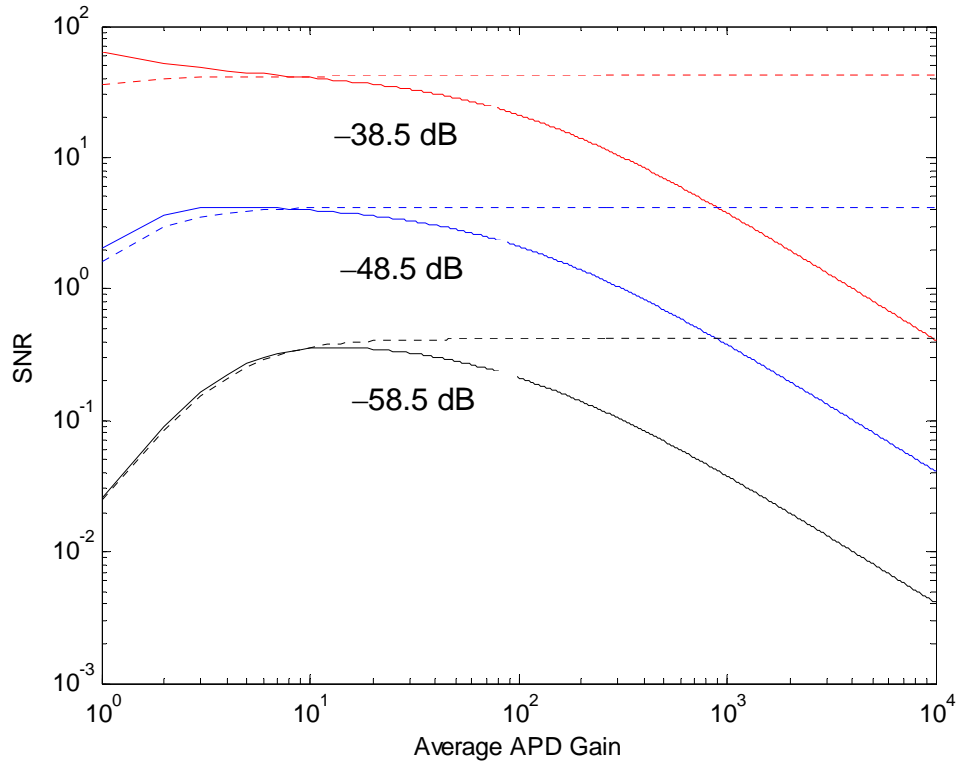
Figure 3-3: SNR versus the average APD Gain. Dotted curves are for fixed value of $F_e = 2$.

Figure 3.4 plots the BER versus number of simultaneous users for optimal value of threshold but with different gains and confirms the results obtained in Fig. 3 that as the value of APD is increased the BER performance is degraded. One can verify that the best bit error rate performance is achieved when the APD with gain around 10 is used.
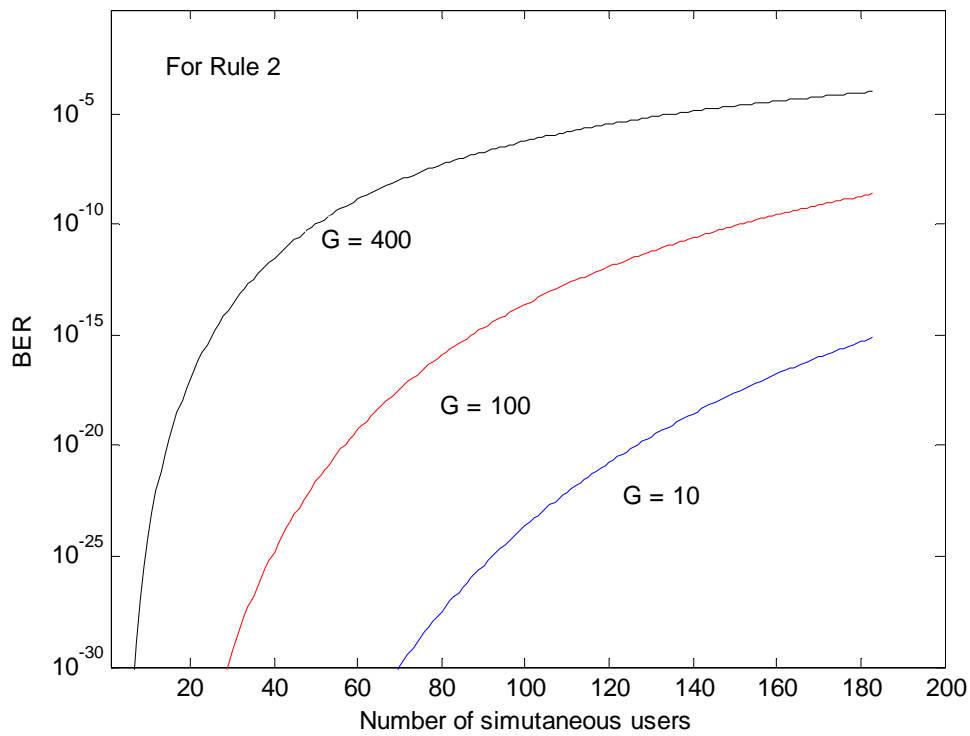
Figure 3-4: BER versus the number of simultaneous users for different values of APD Gain.

The uniformity losses of 0.5 dB and 1.1 dB obtained from the data sheets of practical vendors [56] have been applied in the analysis presented in section 3.3. As can be seen from Figure 3.5 to 3.8, that uniformity loss is a serious problem of the system configured in [5]. Figure 3.5 and 3.6 shows the results for uniformity loss of 0.5 dB and 1.0 dB, for $w = 14$, respectively with the condition of $G_1 = G_2$. While Figure 3.7 and Figure 3.8 shows the BER versus number of active users curve for uniformity loss of 0.5 and 1.0 dB, and k with the condition that $G_2 =$

0.95G_1 and 0.9G_1, respectively. It can be observed from these curves that, the uniformity loss itself is not a serious threat to the PDC based system but when combined with gain mismatch in the information and MAI canceling branch it rapidly degrades the system performance. Considering the gain mismatch and uniformity of splitter loss, it can be seen that the SAC-PDC OCDMA system which applies θ_1 provides best performance because it is suitable for the cases where the statistics for bits '1' and '0' have the same variance.
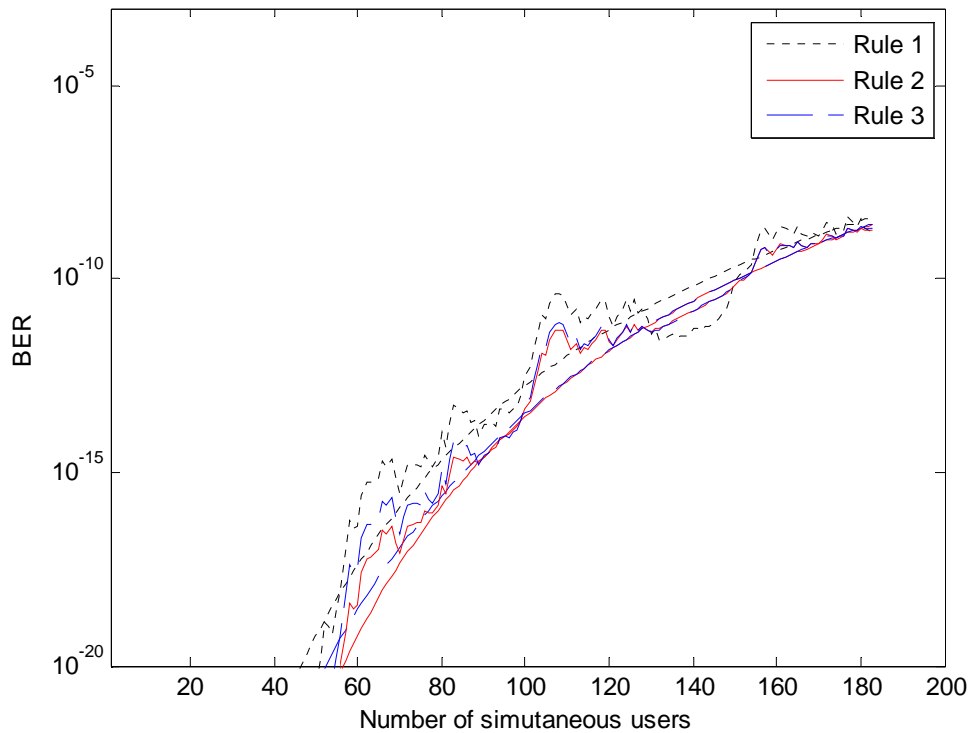
Figure 3-5: BER probability for w = 14 and splitter loss of 0.5 dB.
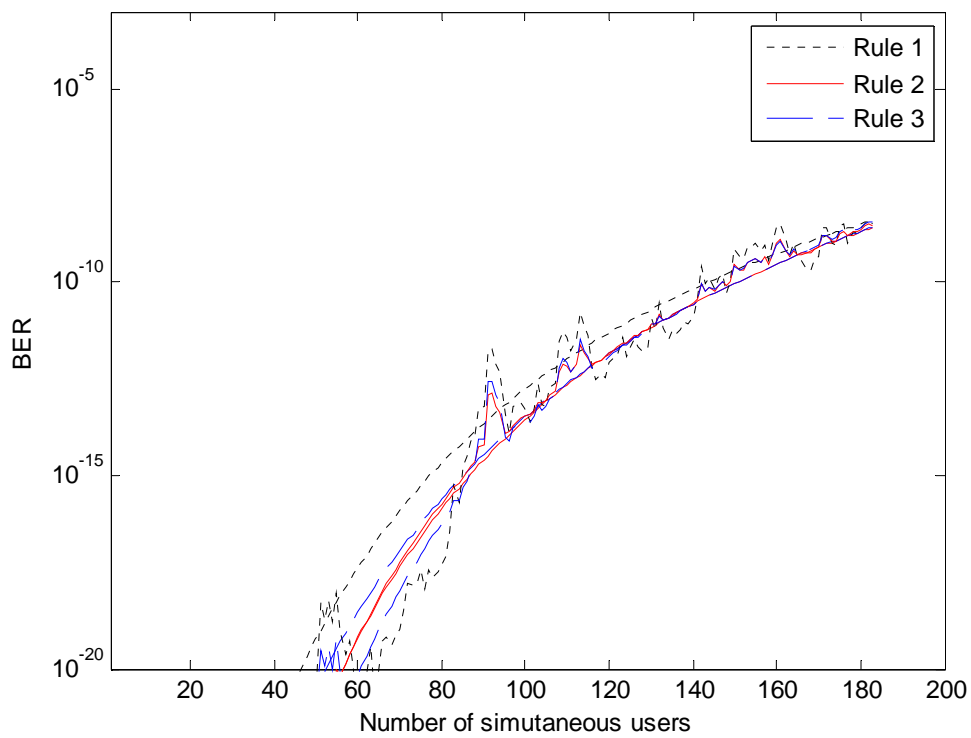
Figure 3-6: BER probability for w = 14 and splitter loss of 1.0.dB.
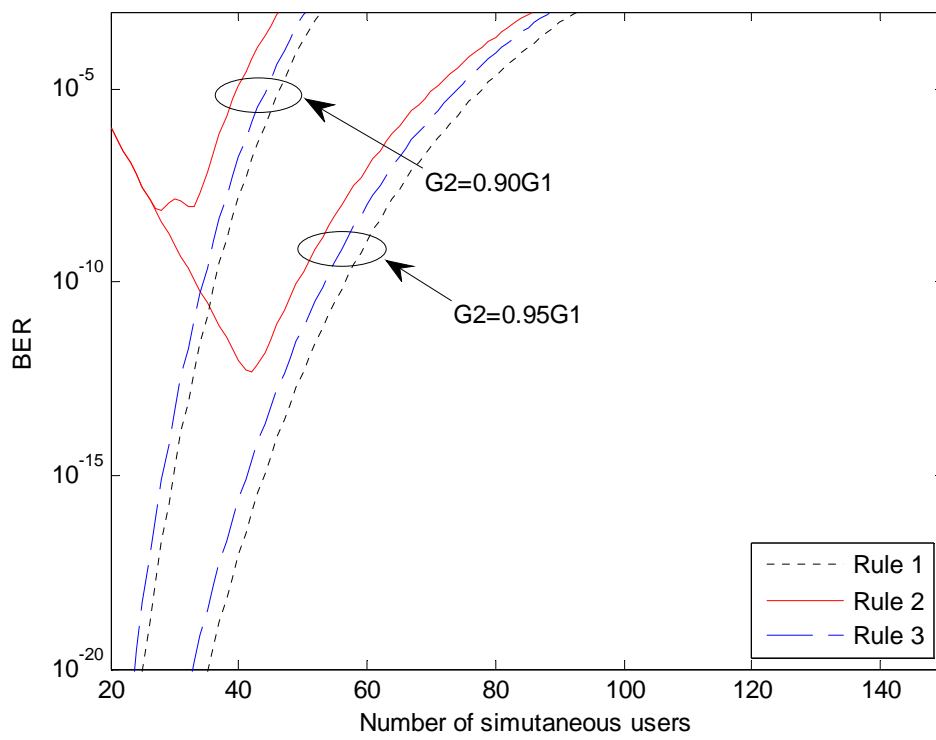
Figure 3-7: BER probability for w = 14 and splitter loss of 0.5 dB.
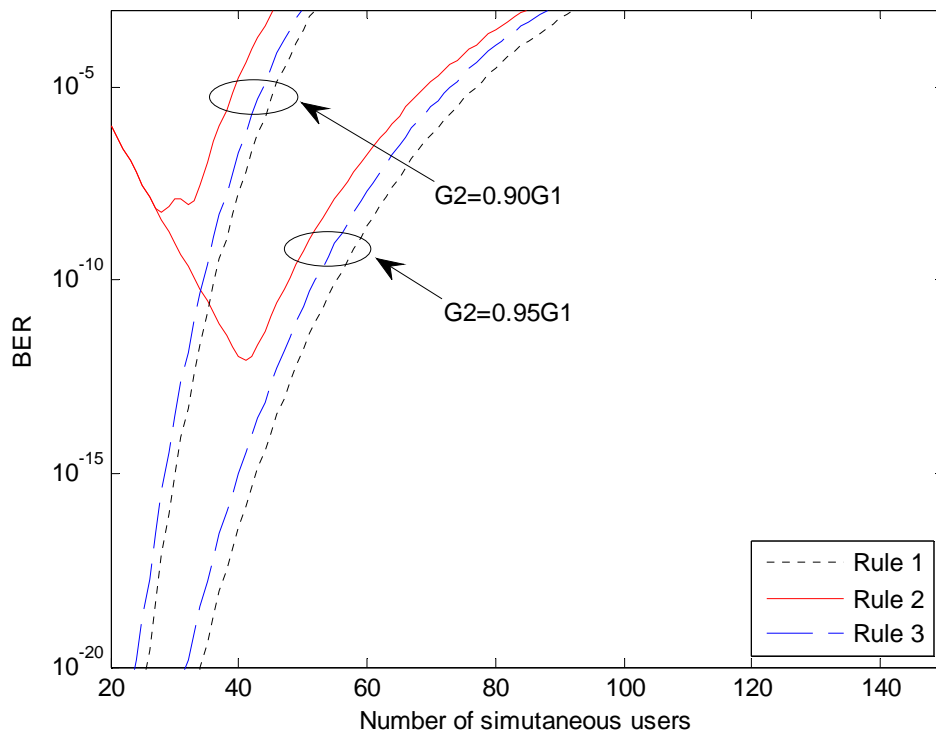
Figure 3-8: BER probability for w = 14 and splitter loss of 1.0.dB.

3.5 Summary

The results show that the system performance is severely affected for the worst when the mismatch losses in the APDs of receiver and splitting losses of the multiplexers are taken into account. On its own the splitter loss can be neglected but when combined with Gain mismatch it degrades the bit error rate performance. This generates the need to explore a better system configuration which can reduce the effect of APD mismatch and uniformity losses. One of the possible solutions for such requirement would be to use balanced sequences.

Alternatively, if the level of interference floor is made fixed, the decoding architecture can be relieved from estimating it over and over again for each data bit decision. This can be achieved using a technique called Common zero codes described in the next chapter. Moreover, it is concluded from experiments that, the effects of other factors such as I_b and I_s, on the system performance are negligible.

4. Compact En/Decoder design for Spectral Amplitude Coding-OCDM System based on Perfect Difference Codes

In this chapter, common zero code technique is introduced and novel encoder/decoder architecture is proposed for spectral amplitude coding, optical code division multiplexing systems. The analytical expressions for signal-to-noise ratio and bit error rate are derived for perfect difference codes structured on the proposed encoding/decoding devices considering, phase-intensity induced noise, thermal noise, and multiple-access interference.

4.1 Introduction

Optical code division multiple-access (OCDMA) technology entered the research field of optical fiber communication in the middle of 1980s and it has offered many advantages such as interfering resistance, asynchronous operation, increased inherent security, and many others. It is particularly found useful for the bursty nature of local area network's environment. Since M. Kaevhrad [42] proposed non-coherent optical CDMA system in 1995, non-coherent spectral-

amplitude coding optical CDMA technology has attracted great deal of attentions from the research point of view.

Several code families can be used in SAC-OCDMA systems, e.g., maximal-length sequence (*m*-sequence) codes [42], Walsh–Hadamard codes [42], modified quadratic congruence codes [52], and perfect difference codes [4, 5], etc. Most of these systems except [4, 5] use Fiber Bragg Gratings (FBGs) as encoding-decoding devices, but FBG array physical size becomes impractical when the number of total network users is large. Such systems change the signature sequence by tuning each FBG piezoelectrically or thermally. Therefore, the configurability of the system is limited by the tuning range of the FBGs [58]. Furthermore, the systems reported in [52, 57] require two sets of FBGs with opposite orders to compensate for the round trip delay of the corresponding spectral components to achieve chip synchronization. This requirement limits the attainable data transmission rate of the system. One way to solve this problem is to use the cyclic property of AWG routers [4, 55] encoder/decoder size reduction.

Different users can use a common code to encode the zero bits [61]. This maintains a constant interference level whether the interfering users are transmitting 1 or 0. Therefore no additional circuitry is required to estimate interference at receiving end rendering the decoding process independent of active number of users and therefore also, simpler and faster. In order to maintain a constant MAI, two different codes are assigned for each channel to encode bit 1 and 0 separately. Moreover, to reduce the number of codes needed, a simple OOK

decoding scheme is used in the receiver to decode the sequence of bit 1 only. Since the sequence of bit 0 is not decoded in the receiver, different channels can use a common code to encode the bit 0; therefore, only one or a few excess codes are needed to encode the bit 0s.

In this chapter, a simple encoder and decoder design is proposed for SAC-optical code division multiplexing (OCDM) systems similar to [59] and [60] utilizing perfect difference codes structured on AWG routers. In [59] however, two AWG multiplexers are required to generate the sequence and its complement. While [60] structures its encoder and decoders on extended perfect difference codes and requires complex decoding structure comprising of three fiber-bragg gratins, three optical circulators, one attenuator, one balanced photodetector, and a delay line. In this proposal, only one encoder is required based on AWG using common zero code technique [61] which is shared by all the network users while at the decoder a simple correlator receiver typical of CDMA systems is proposed to be used. Thus reducing the system cost significantly. The information signal employs ON–OFF keying with low cost incoherent sources, and the AWG router is used to control the amplitude spectra of incoherent optical sources. Because of the cyclic properties of both AWG routers and PDC-sequence codes, the proposed codec pair can encode–decode multiple code words of –sequence code while retaining the ability for MAI cancellation.

Introduction in section 4.1 is followed by system description in section 4.2. It elaborates the encoder and decoder design for spectral amplitude OCDMA

systems based on PDCs only and PDCs with common zero code. In section 4.3, the system performance is analyzed taking into account of intensity noise, shot noise and thermal noise. Additionally, some numerical results are also presented. Finally, this chapter ends with conclusions in section 4.4.

4.2 System Description

4.2.1 PDC Based SAC

Figure 4.1 shows the proposed encoder designed with PDCs for $v = 7$ and $w = 3$. It contains 1×7 splitter and one 7×7 AWG router which can generate seven codewords simultaneously. The AWG router demultiplexes the wavelength into all the output ports, and the same wavelength signals which are incident from different input ports will go to different output ports in cyclic manner [62]:

$$(\#Input\ port + \#Output\ port - 1)\ \text{mod}\ v = \#Wavelength \qquad (4.1)$$

The spectrum of broadband light source is filtered within one free spectral range of the AWG router. After the light is incident on the splitter it is broadcast to 3 specific AWG input ports according to the adopted PDC. By controlling the states of switches with the user's information bits, d_k the encoder can transmit suitable codewords to the end users.
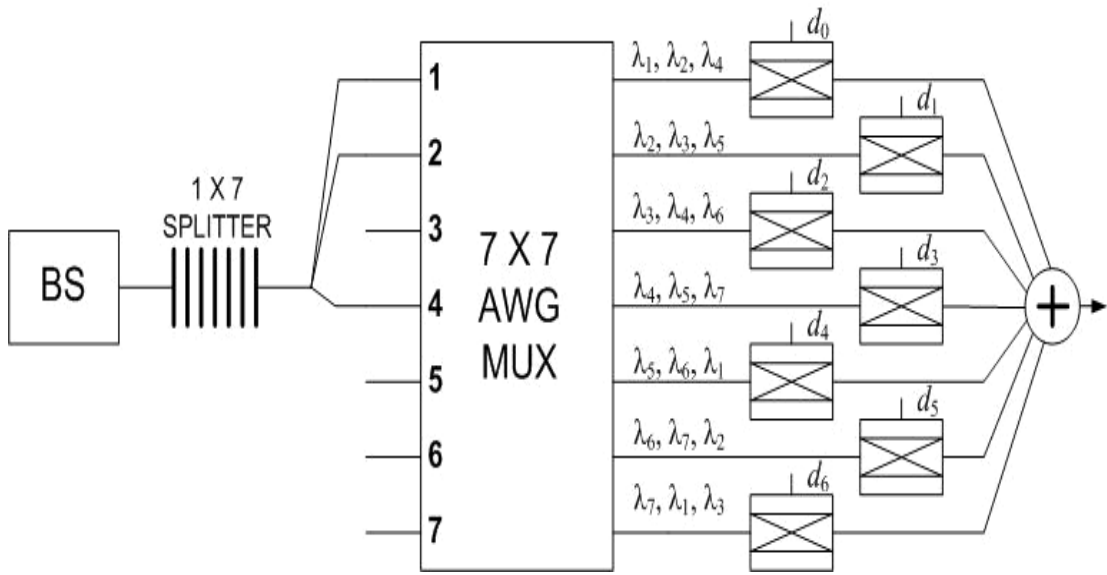
Figure 4-1: Encoder for PDC based SAC-OCDM system (BS: Broadband Source).
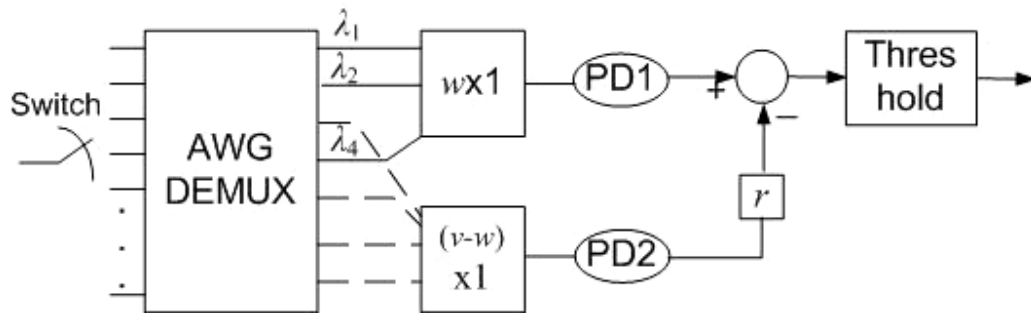
Figure 4-2: Decoder for PDC based SAC-OCDM system.

A $N \times N$ star coupler is assumed to connect the local network users in the system. Each transmitter broadcasts its encoded signal to all the receivers in the network. Figure 4.2 shows the receiver structure similar to that proposed in [5] based on AWGs and PDC sequences. The receiver applies a CDMA correlator to the

incoming signal to extract the desired bit stream. The correlator output consists of the desired data and the unwanted MAI. In order to reduce the effect of MAI, orthogonal codes are required.

A pulse with specified spectral distribution is sent when the data bit is '1', and nothing is sent when the data bit is '0'. At the receiver side, a $N \times N$ multiplexer is used which divides the received signal into two parts. Then they are inputted, respectively, into two decoders with complementary decoding functions. If (v, w, γ) code is used, where v is the length of the code sequence, w is the weight of the code sequence and γ is the correlation constraint, is the MAI coming from $N - 1$ interfering users at the second photodetector (PD2) is equal to $(N - 1)\lambda$ and that at PD1 is equal to $r(w - 1)(K - 1)$. When $r = \lambda / (w - 1)$, these two MAI components are equal and therefore cane be cancelled.

An illustrative example is presented in Table 4,1 for $v = 7$ chips as follows: Assume that User # 2 and User # 6 are to transmit bit '0' while all other users are transmitting data bit '1'. To implement this status of switches d_2 and d_6 in Figure 4.1 will be in BAR state (OFF) while all remaining switches will be in CROSS state (ON). After the encoding, the coded spectral chips are combined in the star coupler and broadcast to each receiver. Each receiver will receive the accumulated signal Rx = (2, 3, 1, 2, 3, 2, 2) as shown in Table 4.1.

Table 4-1: Encoding Scheme for SAC-OCDM System with PDC.

User	Assigned code C_x							Data bit	Transmitted Signal						
#1	1	1	0	1	0	0	0	1	1	1	0	1	0	0	0
#2	1	0	1	0	0	0	1	0	0	0	0	0	0	0	0
#3	0	1	0	0	0	1	1	1	0	1	0	0	0	1	1
#4	1	0	0	0	1	1	0	1	1	0	0	0	1	1	0
#5	0	0	0	1	1	0	1	1	0	0	0	1	1	0	1
#6	0	0	1	1	0	1	0	0	0	0	0	0	0	0	0
#7	0	1	1	0	1	0	0	1	0	1	1	0	1	0	0
Received Signal, Rx =									2	3	1	2	3	2	2

Table 4-2: Decoding Scheme for SAC-OCDM System with PDC.

User # 1: 7 – 8/2 = 3 hence bit detected is '1'									
	Rx	2	3	1	2	3	2	2	
	C_1	1	1	0	1	0	0	0	
Reflected	A	2	3	0	2	0	0	0	7
chips	B	0	0	1	0	3	2	2	8
User # 2: 5 – 10/2 = 0 hence bit detected is '0'									
	Rx	2	3	1	2	3	2	2	
	C_2	1	0	1	0	0	0	1	
Reflected	A	2	0	1	0	0	0	2	5
chips	B	0	3	0	2	3	2	0	10

In order to spectrally decode (see Table 4.2) the kth user's information (we take user #1 and #2 as an example), the received signal vector Rx is directed to the AWG demultiplexer where it is splitted into N spectral components and multiplied by C_1 and $r\overline{C_1}$ to achieve balanced photodetection. For receiver user # 1, the received signal Rx = (2, 3, 1, 2, 3, 2, 2) when correlated with C_1 = (1, 1, 0,

1, 0, 0, 0) and $\overline{C_1}$ = (0, 0, 1, 0, 1, 1, 1) results in the reflected chip vector at A branch with sum = 7 unit powers, and reflected chip vector at B branch with sum = 8 unit powers as shown in Table 4.2. Balanced photodetection will result 7 – 8/2 = 3 units of photocurrent, equivalent to data bit '1'. For user # 2, when the same received signal Rx is correlated with C_2 and $\overline{C_2}$, results in the reflected chip vector at A branch with sum = 5 unit powers, and at B branch with sum = 10 unit powers. Therefore, the balanced photodetection will result 5 – 10/2 = 0 unit powers, corresponding to a detected logical bit of '0'. The decoding process for other receivers can be similarly implemented.

4.2.2 PDC Based SAC with Common Zero Codes

Figure 4.3 shows the proposed encoder designed with PDCs for v = 7 and w = 3. It contains 1×7 splitter and one 7×7 AWG router which can generate seven codewords simultaneously. The spectrum of broadband light source is filtered within one free spectral range of the AWG router. After the light is incident on the splitter it is broadcast to 3 specific AWG input ports according to the adopted PDC. By controlling the states of switches with the user's information bits, d_k the encoder can transmit suitable codewords to the end users. A pulse with specified spectral distribution is sent when the data bit is '1', and common code is sent for all the users when the data bit is '0'.
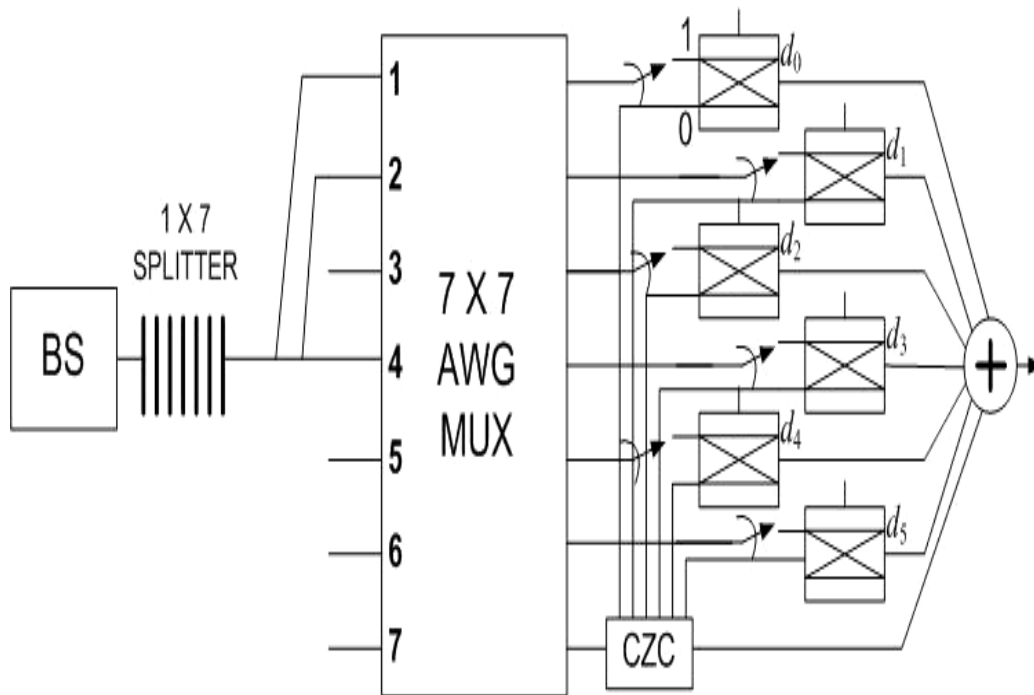
**Figure 4-3:** Encoder for SAC-OCDMA system based on PDC. (BS: Broadband Source)
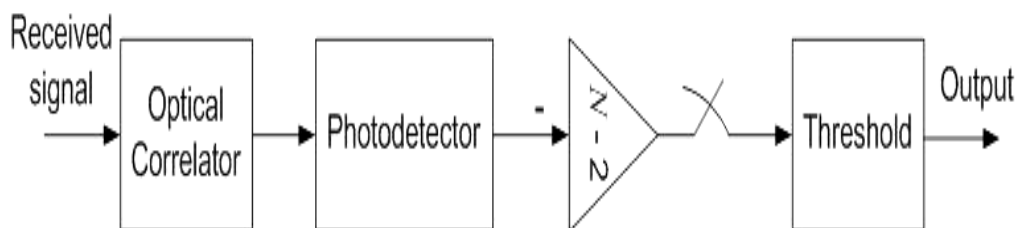
Figure 4-4: Decoder for SAC-OCDMA system with Common Zero Code.

A $N \times N$ star coupler is assumed to connect the local network users in the system. Each transmitter broadcasts its encoded signal to all the receivers in the network. Figure 4.4 shows the receiver structure based on AWGs and PDC sequences. The

receiver applies a CDMA correlator for C_k (code for kth user) to the incoming signal to extract the desired bit stream. The correlator output simply consists of the desired data as opposed to conventional receiver structures used for SAC which require MAI cancellation branch as well along with information branch as explained in last section. After the correlation the signal is detected by photodetector. Since each other user in the system will contribute one spectral component in the desired user's bit stream, their contribution is subtracted with a constant factor of $(N - 2)$. The factor $N - 2$ arises because out of total N spreading codes only $N - 1$ can be assigned and one is reserved for common zero code. This arrangement does not need to estimate the interference in order to cancel it from the desired signal.

Table 4-3: Encoding Scheme for SAC-OCDM system with PDC-CZC.

User	Assigned code C_x							Data bit	Transmitted Signal						
#1	1	1	0	1	0	0	0	1	1	1	0	1	0	0	0
#2	1	0	1	0	0	0	1	0	0	1	1	0	1	0	0
#3	0	1	0	0	0	1	1	1	0	1	0	0	0	1	1
#4	1	0	0	0	1	1	0	1	1	0	0	0	1	1	0
#5	0	0	0	1	1	0	1	1	0	0	0	1	1	0	1
#6	0	0	1	1	0	1	0	0	0	1	1	0	1	0	0
#7 CZC	0	1	1	0	1	0	0	1	-	-	-	-	-	-	-
Received Signal, Rx =									2	4	2	2	4	2	2

Table 4-4: Decoding Scheme for SAC-OCDM system with PDC-CZC.

User # 1: 8 – 5 = 3 hence bit detected is '1'								
Rx	2	4	2	2	4	2	2	
C_1	1	1	0	1	0	0	0	
Reflected chips	2	4	0	2	0	0	0	8
User # 2: 6 – 5 = 1 hence bit detected is '0'								
Rx	2	4	2	2	4	2	2	
C_2	1	0	1	0	0	0	1	
Reflected chips	2	0	2	0	0	0	2	6

An illustrative example is presented in Table 4.3 and 4.4 for $N = 7$ chips as follows: Assume that User # 2 and User # 6 are to transmit data bit '0' while all other users are transmitting data bit '1'. Since user #2 and user # 6 are transmitting zero they will be assigned the Code # 7 as common code instead of code # 2 and #6 as shown in Table 4.3. To implement this status of switches d_2 and d_6 in Figure 4.3 will be BAR and directed to Code #7, while all remaining switches will be CROSS and will be transmitting their respective codes. After the encoding, the coded spectral chips are combined in the star coupler and broadcast to each receiver. Each receiver will receive the accumulated signal Rx = (2, 4, 2, 2, 4, 2, 2) as shown in Table 4.3. Please note that here penalty of one user is paid due to the common zero code.

In order to spectrally decode (see Table 4.4) the kth user's information (assuming user #1 as desired user), the received signal vector Rx is splitted into N spectral components and multiplied by C_1 only to achieve photodetection. For receiver user # 1 the reflected chip vector has sum = 8 unit powers. Since the total number of interfering chips for each user is fixed that is $N – 2 = 5$, where N is the number

of active users, the photodetection will result $8 - 5 = 3$ units of photocurrent, equivalent to data bit '1'. For user # 2, the reflected chip vector sum = 6 unit powers, therefore, photodetection will result $6 - 5 = 1$ unit powers, corresponding to a detected logical bit of '0'. The decoding process for other receivers can be similarly implemented.

4.3　Performance Analysis

In the analysis of proposed system, noises that exist in this system contain shot noise, incoherent phase-induced intensity noise (PIIN) and thermal noise. The effect of the receiver's dark current is assumed to be neglected. Gaussian approximation is used for the calculation of bit error rate.

The light source spectra are assumed to be ideally unpolarized and ideally flat over a Δv bandwidth, with magnitude $P/\Delta v$, where $P = P_{sr}$ is the effective source power. Therefore, the variance of photocurrent due to the detection of an unpolarized thermal light, which is generated by spontaneous emission, can be denoted as [45]:

$$\langle i^2 \rangle = 2eI_p B + I^2 B \tau_c + 4 K_b T_n B / R_L \qquad (4.2)$$

where e is the electron charge, I_p is the photocurrent, B is the electrical bandwidth of the receiver, K_b is the Boltzmans constant, T_n is the receiver noise temperature, R_L is the load resistance, and τ is the source coherence time expressed in [63]:

$$\tau_c = \frac{\int_0^\infty G^2(v)dv}{\left[\int_0^\infty G(v)dv\right]^2} \qquad (4.3)$$

where the $G(v)$ is assumed to be single sideband power spectral density (PSD) of the source. The first term of Equation 4.2 denotes the shot noise, while the second and the third term represent the effect of PIIN and thermal noise respectively.

Let $c_k(i)$ denote the ith element of the kth PDC code. The code properties can be written as:

$$\sum_{i=1}^{v} c_k(i)c_l(i) = \begin{cases} w, & k = l \\ 1, & k \neq l \end{cases} \qquad (4.4a)$$

$$\sum_{i=1}^{v} c_k(i)\overline{c_l}(i) = \begin{cases} 0, & k = l \\ w-1, & k \neq l \end{cases} \qquad (4.4b)$$

Thus, the power spectral density (PSD) of the received optical signal can be written as:

$$P_r = \frac{P}{\Delta v} \sum_{k=1}^{K} \sum_{i=1}^{v} [d_k c_k(i)]\{rect(i)\} \qquad (4.5)$$

4.3.1 Performance Analysis of PDC Based SAC

Assuming the bit synchronization between transmitter and receiver, the PSD at PD1 and PD2 (see Figure 4.1 and 4.2) of the lth user receiver during one bit period can be written as.

$$G_1(v) = \frac{P}{\Delta v} \sum_{k=1}^{K} b_k \sum_{i=1}^{v} c_k(i) c_l(i) \{rect(i)\} \tag{4.6}$$

and

$$G_2(v) = r \frac{P}{\Delta v} \sum_{k=1}^{K} b_k \sum_{i=1}^{b} c_k(i) \overline{c_l}(i) \{rect(i)\} \tag{4.7}$$

Using formulae (4.3), (4.6) and (4.7), the total power incident on PD1 and PD2 is given by,

$$\int_0^\infty G_1(v) dv = \frac{P}{v}(w + K - 1) \tag{4.8}$$

and

$$\int_0^\infty G_2(v) dv = r \frac{P}{v}(K - 1)(w - 1) \tag{4.9}$$

Since $r = 1/(w - 1)$

$$\int_0^\infty G_2(v) dv = \frac{P}{v}(K - 1) \tag{4.10}$$

Therefore, using formulae (4.6) and (4.7), we can obtain

$$\int_0^\infty G_1^2(v) dv = \frac{P_s^2}{v \Delta v} \cdot \sum_{i=1}^{v} \left\{ c_l(i) \left[\sum_{k=1}^{K} b_k c_k(i) \right] \left[\sum_{s=1}^{K} b_s c_s(i) \right] \right\} \tag{4.11}$$

69

$$\int_0^\infty G_2^2(v)dv = r^2 \frac{P^2}{N\Delta v} \cdot \sum_{i=1}^{N} \left\{ \left[\sum_{k=1}^{K} d_k c_k(i) \right] \left[\sum_{s=1}^{K} d_s c_s(i) \right] \overline{c_l(i)} \right\} \qquad (4.12)$$

The photocurrent I_p can be expressed as:

$$I_p = I_1 - I_2 = \Re \frac{P}{v} w b_k \qquad (4.13)$$

where $\Re = (\eta e)/(hf)$ is the responsivity of the photodetector. Here, η is the quantum efficiency, e is the electron's charge, h is the plank's constant, and f is the central frequency of the original broad-band optical pulse. Due to the noise at PD1 and PD2 which are independent, the power of noise sources in the photocurrent can be written as

$$\langle i^2 \rangle = 2eB(I_1 + I_2) + BI_1^2 \tau_{c1} + BI_2^2 \tau_{c2} + 4K_b T_n B / R_L \qquad (4.14)$$

When all users are transmitting data bit '1', on average we can approximate $\sum_{k=1}^{K} c_k(i) \approx K/(w-1)$. Using the correlation properties, the noise power can be written as

$$<i^2> = \frac{2eB\Re P[w + 2(K-1)]}{v} + \frac{B\Re^2 P^2 Kw(w+K-2)}{v\Delta v(w-1)^2}$$
$$+ 4K_b T_n B / R_L \qquad (4.15)$$

Note that the probability of sending '1' at any time for each user is 1/2, the above equation becomes

$$< i^2 > \cong \frac{eB\Re P[w + 2(K-1)]}{v}$$
$$+ \frac{B\Re^2 P^2 Kw(w + K - 2)}{2v\Delta v(w-1)^2} + 4K_b T_n B / R_L \tag{4.16}$$

From (4.11) and (4.16), the expression for SNR can be derived as in (4.17).

$$SNR_{PDC} = \frac{\Re^2 P^2 w^2 / v^2}{\frac{eB\Re P[w + 2(K-1)]}{v} + \frac{B\Re^2 P^2 Kw(w + K - 2)}{\left(2v\Delta v(w-1)^2\right)} + 4K_b T_n B / R_L} \tag{4.17}$$

4.3.2 Performance Analysis of PDC Based SAC with Common Zero Codes

Assuming bit synchronization, the PSD at PD (see Figure 4.3 and 4.4) of the lth user receiver during one bit period can be written as

$$G(v) = \frac{P}{\Delta v} \sum_{k=1}^{K} \sum_{i=1}^{v} [d_k c_k(i)] c_l(i) \{rect(i)\} \tag{4.18}$$

Using formula (4.4), the total power incident on PD is given by

$$\int_0^\infty G(v) dv = \frac{P}{v} w b_l \tag{4.19}$$

Therefore, using formulae (4.18), we can obtain

$$\int_0^\infty G^2(v)dv = \frac{P^2}{v\Delta v} \cdot \sum_{i=1}^v \left\{ \left[\sum_{k=1}^K b_k c_k(i) \right] \left[\sum_{s=1}^K b_s c_s(i) \right] c_l(i) \right\} \tag{4.20}$$

The photocurrent I can be expressed as

$$I = R\int_0^\infty G(v)dv = \frac{\Re P}{v}wb_l \tag{4.21}$$

Due to the noise at PD which are independent, the power of noise sources in the photocurrent can be written as

$$<i^2> = \frac{2eB\Re Pw}{v} + \frac{B\Re^2 P^2(w+K^2-1)}{v\Delta v(w-1)} + 4K_b T_n B/R_L \tag{4.22}$$

Note that the probability of sending '1' at any time for each user is 1/2, the above equation becomes

$$<i^2> = \frac{eB\Re Pw}{v} + \frac{B\Re^2 P^2(w+K^2-1)}{2v\Delta v(w-1)} + 4K_b T_n B/R_L \tag{4.23}$$

From (4.21) and (4.23), we can get the expression for SNR which is shown in (4.24).

$$SNR_{PDC\_CZC} = \frac{\Re^2 P^2 w^2 / v^2}{\dfrac{eB\Re Pw}{v} + \dfrac{B\Re^2 P^2(w+K^2-1)}{(2v\Delta v(w-1))} + 4K_b T_n B/R_L} \tag{4.24}$$

Using Gaussian approximation, the BER can be expressed as:

$$BER = \frac{1}{2} erfc\left(\sqrt{SNR/8}\right) \tag{4.25}$$

On employing this expression (4.25), the relations between the bit error rate and the number of active users for m-sequences, Hadamard codes, complementary Walsh-Hadamard codes [62] of length 128, modified quadratic congruence codes [52] of length 132 and $p = 11$, Perfect Difference Codes of length 133 and weight $w = 12$ with and without application of common zero code are plotted in Figure 4.5. The parameters used in our analysis are listed in Table 4.5. It is worth noting that when properly synchronized the Perfect difference codes and MQC codes due to their unity cross-correlation only contribute the one overlap per interfering user while m-sequences and Hadamard codes causes $(N + 1)/4$ and $N/4$, respectively.
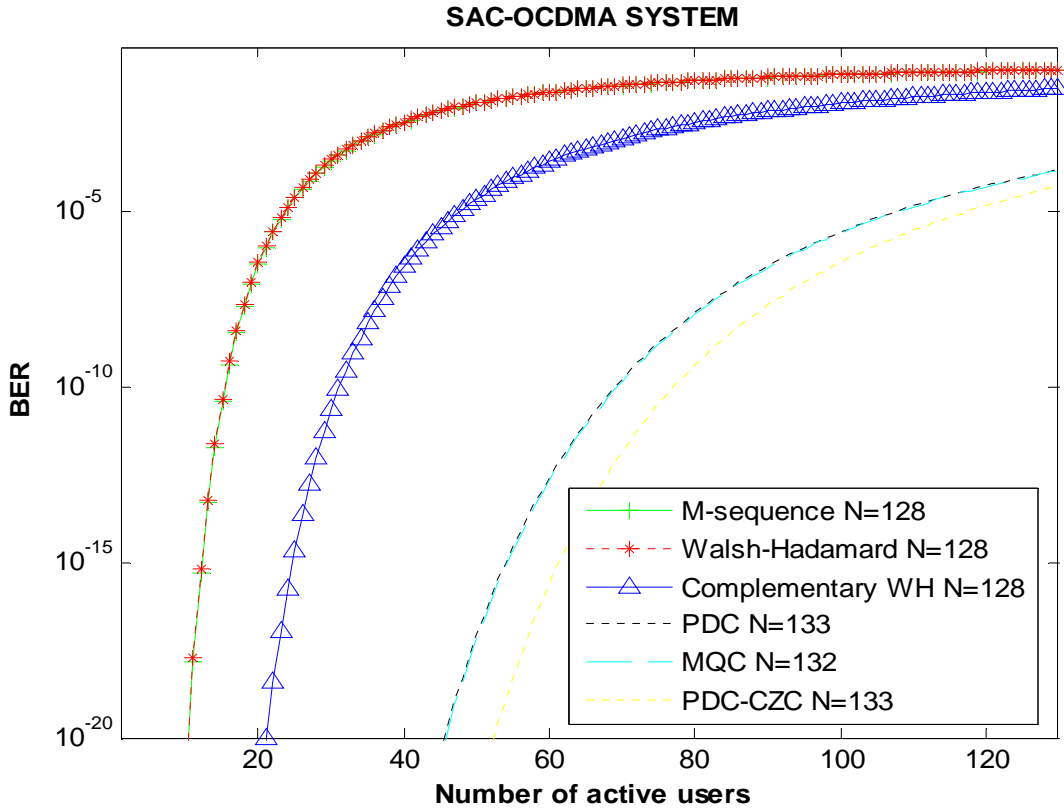
Figure 4-5: BER versus number of active users for different codes.

Table 4-5: Parameters used.

PD quantum efficiency	$\eta = 0.6$
Line-width of the thermal source	$\Delta v = 6.25THz$
Operating wavelength	$\lambda_0 = 1.55\mu m$
Electrical bandwidth	$B = 80MHz$
Receiver noise temperature	$T_r = 300K$
Receiver load resistor	$R_L = 1030\Omega$

Thus, the influence of other users in the network on the desired signal is greatly

reduced, eventually resulting in improved bit-error rate performance which is

more pronounced and obvious to note in Figure 4.5 under heavy loads. The performance of MQC and PDC codes is almost equivalent because both have unity cross correlation, but the later has the advantage of being cyclic and has no constraint of length being a prime number. This renders the implementation of PDCs with common zero codes simpler and efficient. The use of CZC only expense one penalty of code as it is dedicated for the data bit '0' for each user in the system. It is evident from Figure 4.5 that the performance of PDCs can further be improved with the application of CZC because the level of interference contributed by undesired users is constant and therefore eliminating them is relatively easy.

Figure 4.6 shows the relation between the number of simultaneous users and the SNR for different spreading codes with similar lengths as given in Figure 4.5. It has been shown that PDC code gives a much higher SNR than m-sequence or Walsh-Hadamrd codes and have equivalent performance with MQC. While the SNR is further improved if PDC is combined with CZC. Therefore, PDC codes can effectively suppress the effect of intensity noise, resulting in a much better performance.
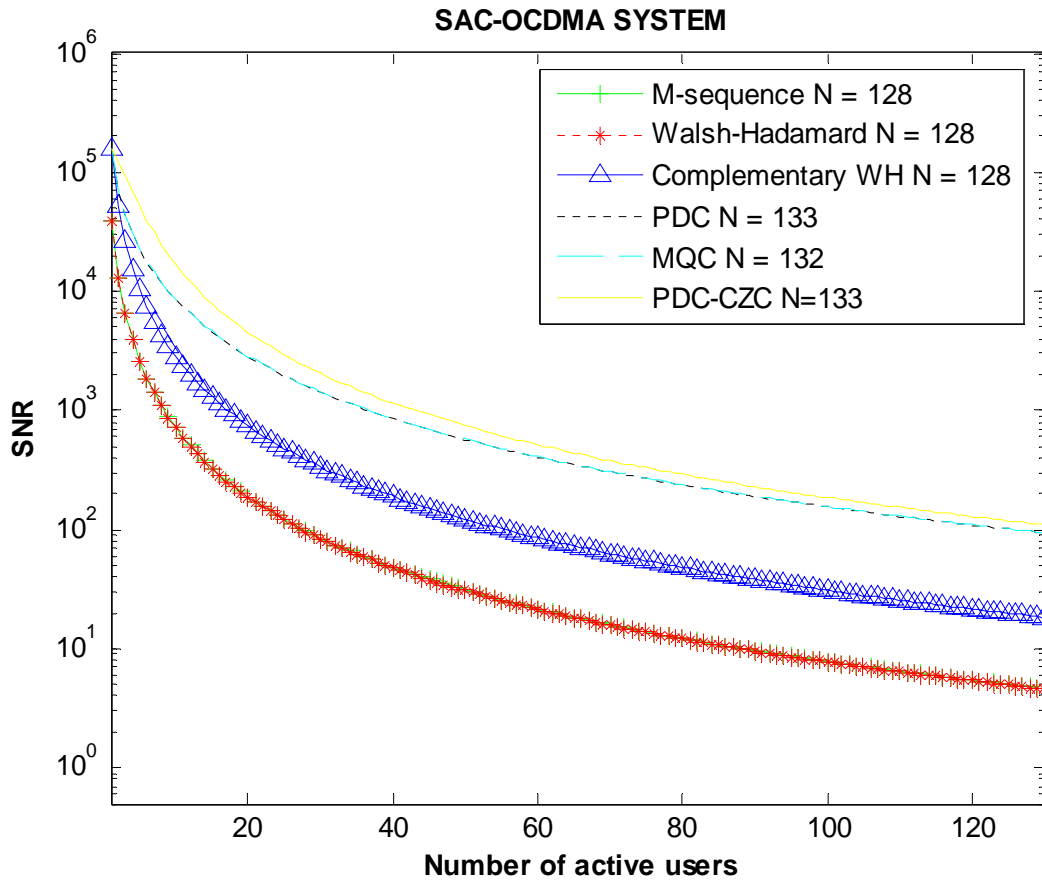
Figure 4-6: SNRs versus number of active users when P = − 10 dBm.

Figure 4.7 shows the variations of BER versus the number of active users when *P* = − 10 dBm for PDCs with and without application of CZC with weights 7, 13, and 20. It is evident from this plot that CZC improve the performance of the system.
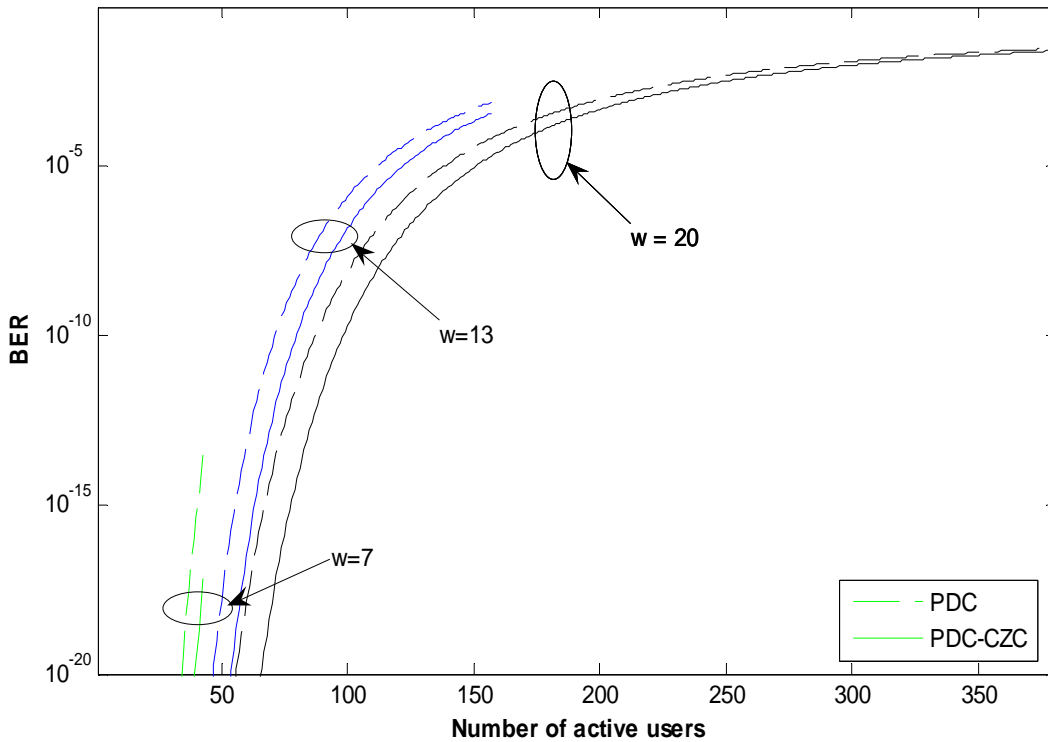
Figure 4-7: BER versus number of active users when P = – 10 dBm.

Figure 4.8 shows the BER variations with the effective power when and the number of simultaneous users is 43. The solid lines represent the BERs, taking into account effects of intensity, shot, and thermal noises. The dashed lines indicate the BER performances when effects of only intensity and thermal noises are considered. The dotted lines indicate the system BERs when only intensity and shot noise sources are considered. It is shown that, when P is large, both the shot and thermal noises are negligibly small compared with the intensity noise, which becomes the main limitation factor of the system performance. However, when P is low, the effect of intensity noise becomes minimal, and, hence, the thermal noise source becomes the main factor that limits the system performance.

77

It is also shown that thermal noise is much more influential than shot noise on system performance.
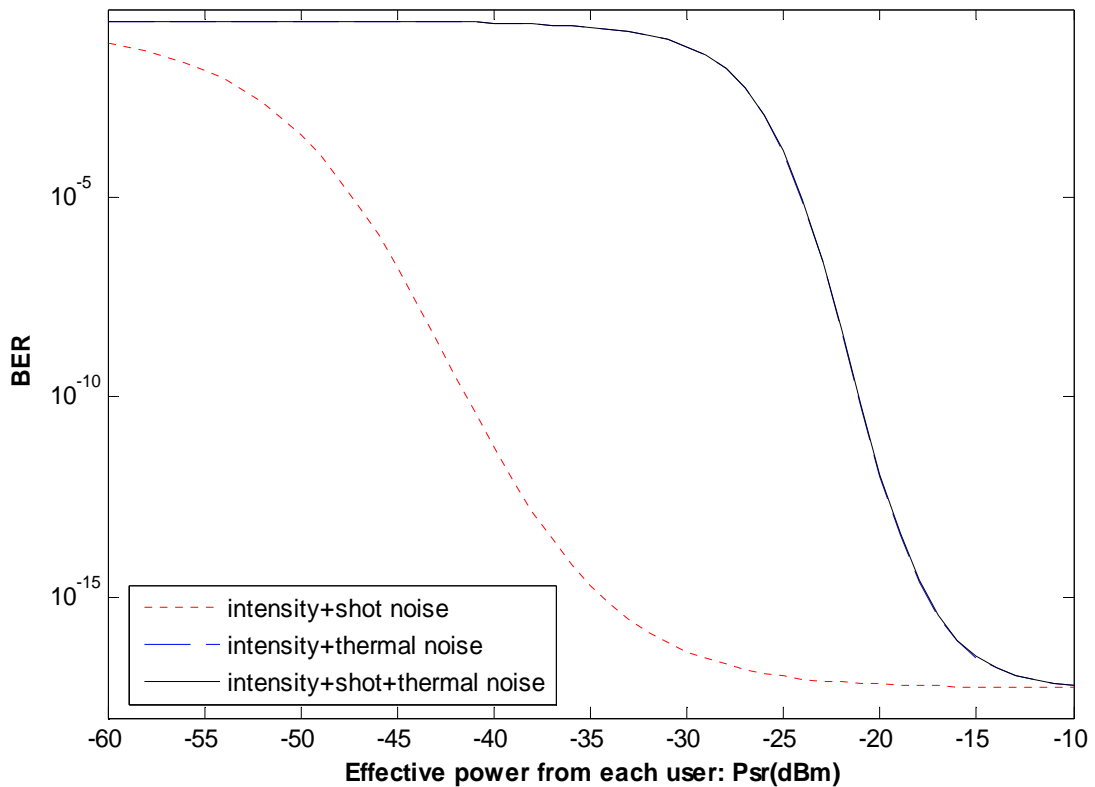
Figure 4-8: BER versus effective power P when number of active users is 43.

Figure 4.9 shows the BER variations with when the number of simultaneous users is 43 and $w = 7$, $w = 13$, and $w = 20$. Figure 4.10 shows variations of the BER versus number of simultaneous users for different values of P. In these two figures, we have considered effects of the intensity, shot, and thermal noise sources. It is shown that when P_{sr} is less than -25 dBm the performance of the

proposed system is poor. This is because the larger value of weight causes a large

power loss at the transmitter.
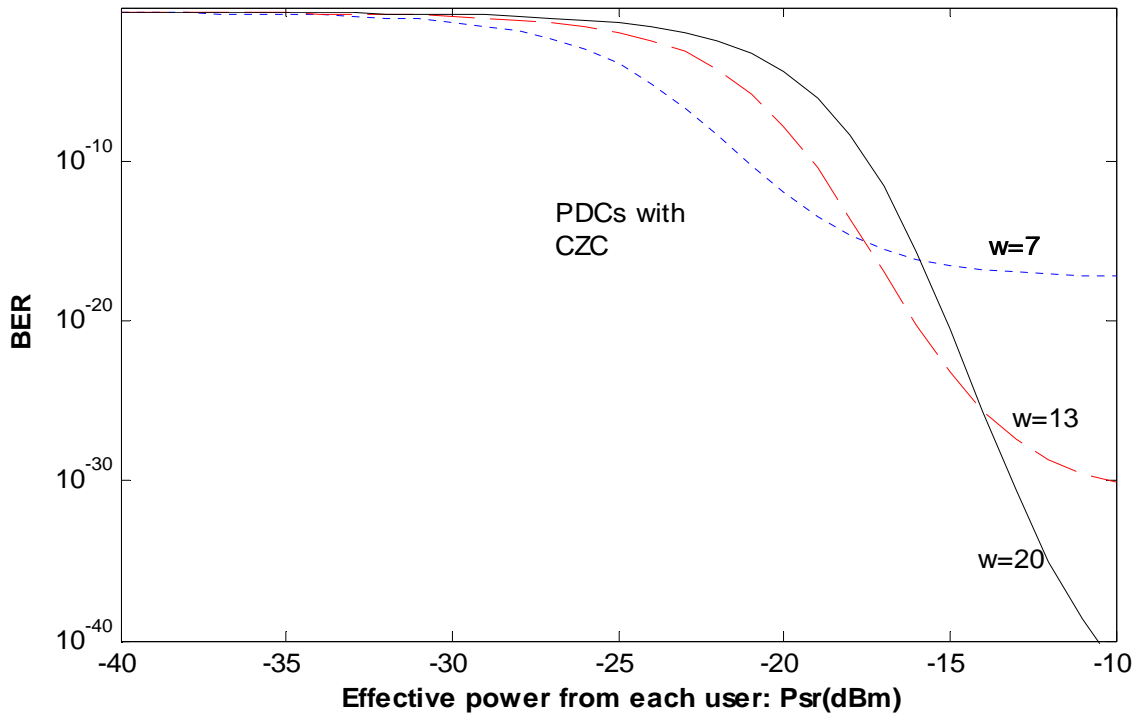
Figure 4-9: BER versus effective power P when number of active users is 43, taking into account the intensity noise, shot noise, and thermal noise.
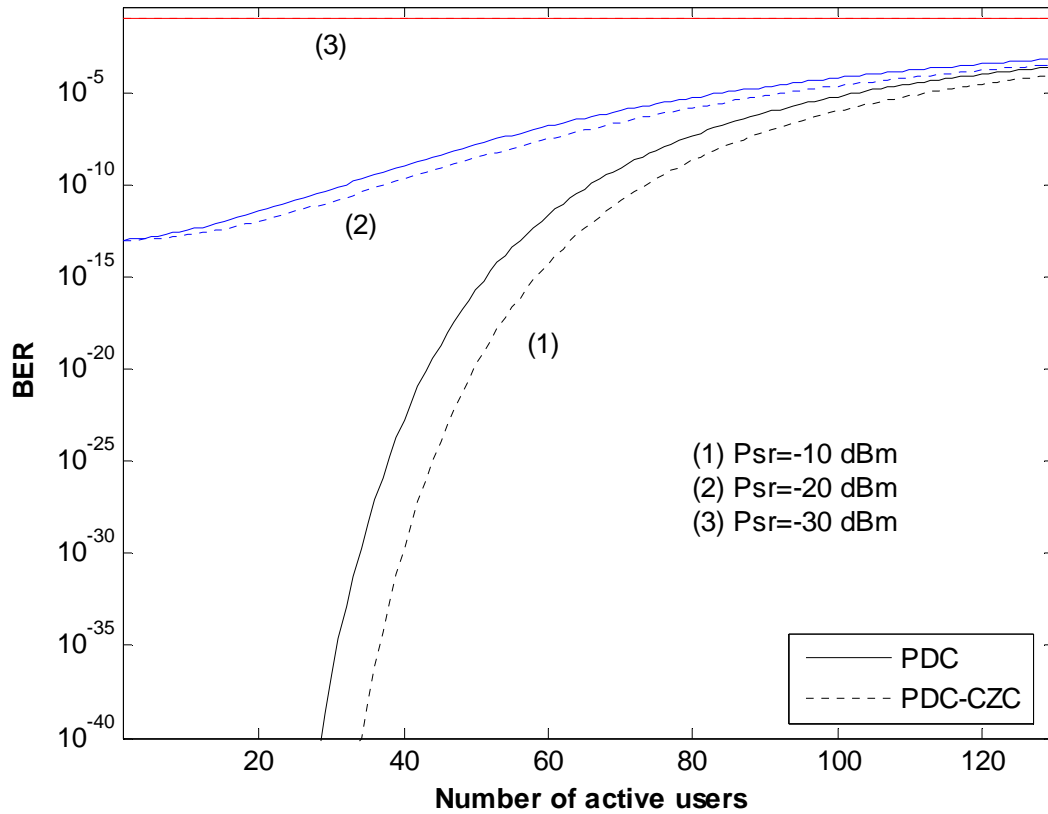
Figure 4-10: BER versus number of active users when effective power P is different.

4.4 Summary

A simple and robust encoder and decoder based on AWG router and simple correlator receiver has been proposed that for the spectral-amplitude OCDMA receiver. Because of the cyclic properties of AWG routers and perfect difference codes, all users can share the same encoder. The bit error rate performance of the SAC-OCDMA system with different codes has been analyzed by taking into account the effects of the shot noise, PIIN and thermal noise. It has been shown that performance levels can be achieved that are greater than the performance

limit of the system employing *m*-sequences, Walsh-Hadamard, and complementary-WH codes and even with MQC codes when employed PDCs with common zero code technique. Low-cost light sources can be used for actual implementation, rendering the network cheap and compact. When flattened sources are used, transmitted data bit can be recovered without the influence of MAI.

The proposed encoding/decoding architecture presents the following advantages:

1. A single AWG multiplexer encoder can be shared by all the users in the network.

2. The introduction of common zero code maintains a constant interference level at all instants in a OCDM network, therefore, at the decoder of each user, the circuitry to estimate the interference is not required. Hence, the speed of data processing and complexity of decoding architecture is significantly improved.

3. Because the CZC enables simple correlation receiver, the typical problem of mismatches in the two branches of typical spectral amplitude system as described in chapter 2 and 3 are non-existent. And the effects of gain mismatch can be ignored.

5. Manchester-Coded Modified-Legendre Sequences

In this chapter, a new family of spreading sequences called Manchester-coded Modified-Legendre sequences is presented.

5.1 Introduction

Yang in [59] proposes modified Legendre sequences for spectral-amplitude coding OCDMA system. Taking the lead from [64], in this chapter Manchester coding is applied to the already modified Legendre sequences and present a new family of sequences called Manchester-coded Modified Legendre Codes (MCMLCs). MCMLCs with complementary coding ability are proposed for SAC OCDM systems. The Manchester coding of MLCs make them suitable for both single rate and Multirate systems ensuring higher quality of service as explained later in this chapter.

The performance of the proposed system is evaluated with respect to multiple-access interference, surface leakage current, background noise and thermal noise to demonstrate that the proposed system can operate efficiently in case of low signal power.

5.2 Modified Legendre Sequences

The modified Legendre (ML) sequences are generated from the well-known binary Legendre or quadratic residue sequences [4]. Let C_v with lengths v be the ML sequences (v is a prime such that $v \equiv 3 \pmod 4$), the corresponding elements are obtained as [59]:

Table 5-1: Modified-Legendre Sequences.

	C_v								$\overline{C_v}$							
$k=0$	0	0	0	1	0	1	1	1	1	1	1	0	1	0	0	0
$k=1$	1	0	0	0	1	0	1	1	0	1	1	1	0	1	0	0
$k=2$	1	1	0	0	0	1	0	1	0	0	1	1	1	0	1	0
$k=3$	0	1	1	0	0	0	1	1	1	0	0	1	1	1	0	0
$k=4$	1	0	1	1	0	0	0	1	0	1	0	0	1	1	1	0
$k=5$	0	1	0	1	1	0	0	1	1	0	1	0	0	1	1	0
$k=6$	0	0	1	0	1	1	0	1	1	1	0	1	0	0	1	0

$$C_{v,i} = \begin{cases} c_{v,i}, & \text{if } 0 \le i \le v-1 \\ 1, & \text{if } i = v \end{cases} \tag{5.1}$$

The elements of complementary codewords are obtained as $\overline{C_{v,i}} = 1 - C_{v,i}$ Thus,

$$C_a \cdot C_b = \sum_i c_{a,i} c_{b,i} = \begin{cases} \dfrac{v}{2}, & \text{if } a = b \\ \dfrac{v}{4}, & \text{if } a \ne b \end{cases} \tag{5.2}$$

Table 5.1 shows the Modified Legendre sequences and their complement for length 8. The original length of Legendre sequences is 7 and the bit 1 and 0 is stuffed into original sequence C_v and its complement to create Modified

Legendre sequences [59]. The stuffed bits are highlighted by the gray shaded area in Table 5.1.

5.2.1 Elementary MCMLCs

The Manchester code is used to represent the each chip. Applying Manchester coding we use '01' and '10' to represent the chip '0' and chip '1', respectively. For simplicity, each 'sub-chips' is regarded as 'chips' and denote the MCMLCs as:

$$C_v^j = \left(c_1^j, c_2^j, \ldots c_{2v}^j \right) \tag{5.3}$$

where $j \in \{1, 2, \ldots, v\}$ and $c_i^j \in \{0, 1\}$ for all $i \in \{1, 2, \ldots, v\}$. Hence the length of MCMLCs is $L = 2v$ while the weight is equal to $w = v$. Table 5.2 shows the Manchester-coded Modified Legendre sequences for length $v = 8$ and C_v. In similar fashion the complement of C_v can be encoded.

Table 5-2: Manchester coded Modified Legendre Sequences.

C_v																
$k=0$	0	1	0	1	0	1	1	0	0	1	1	0	1	0	1	0
$k=1$	1	0	0	1	0	1	0	1	1	0	0	1	1	0	1	0
$k=2$	1	0	1	0	0	1	0	1	0	1	1	0	0	1	1	0
$k=3$	0	1	1	0	1	0	0	1	0	1	0	1	1	0	1	0
$k=4$	1	0	0	1	1	0	1	0	0	1	0	1	0	1	1	0
$k=5$	0	1	1	0	0	1	1	0	1	0	0	1	0	1	1	0
$k=6$	0	1	0	1	1	0	0	1	1	0	1	0	0	1	1	0

Complementary coding us used to transmit data bit 1 and data bit 0. To transmit data bit '1', we use the MCMLCs C_L^j and to transmit data bit '0' we use $\overline{C_L^j}$. For such systems these are the properties of the MCMLCs.

1. Correlation between two MCML sequences

$$C_a \cdot C_b = \sum_i c_{a,i} c_{b,i} = \begin{cases} \dfrac{L}{2}, & \text{if } a = b \\ \dfrac{L}{4}, & \text{if } a \neq b \end{cases} \tag{5.4}$$

2. Correlation between sequences and its complement.

$$C_a \cdot \overline{C_b} = \sum_i c_{a,i} \overline{c_{b,i}} = \begin{cases} 0, & \text{if } a = b \\ \dfrac{L}{4}, & \text{if } a \neq b \end{cases} \tag{5.5}$$

3. Each transmitted bit, whether it is transmitting 1 or 0, always contributes $L/2$ marked chips during one bit interval.

5.2.2 Extended MCMLCs

In this subsection, the elementary MCMLC C_L^j is extended by copying every chip to 2^E chips and denote the extended MCMLC as $_E C_L^j$. For example, some codes of the families for modified-Legendre sequence $(001|1, \ v = 4)$ are listed in Table 5.3.

It is important to note that the code length and weight of the extended MCML code $_{E}C_{L}^{j}$ are now $2^{E+1}v$ and $2^{E}v$, respectively. However, it retains all the properties of MCMLCs.

Table 5-3: Extended MCMLCs with (001|1).

		E = 0	E = 1	E = 2
v = 4	i=1	01011010	0011001111001100	00001111000011111111000011110000
	i=2	10010110	1100001100111100	11110000000011110000111111110000
	i=3	01100110	0011110000111100	00001111111100000000111111110000

By the properties of MCMLCs, the self inner product in the $_{E}C_{L}^{j}$ user is equal to $2^{E}v$ and the interference contributed by every other user is equal to $2^{E-1}v$. The extended MCMLCs can be used for single rate or multi-rate systems. To support demanding users, the sequences with lower values of (e.g., E = 0) can be assigned, while the other users with nominal data rate, the sequences with higher E can be assigned.

5.3   System Description

Figure 5.1 shows the structure of encoder based on MCMLC. It consists of two optical encoders C_{L}^{j} and $\overline{C_{L}^{j}}$ to encode bit 1 and bit 0, respectively. In the proposed OCDMA system, the transmitted data is optically encoded according to an MCMLC or its complement in the transmitter, and the received signal is decoded according to the same MCMLC. Without loss of generality, we restrict our discussion to the user that uses $_{0}C_{L}^{j}$ (we denote it as C_{L}^{j} for simplicity) as the spreading code.
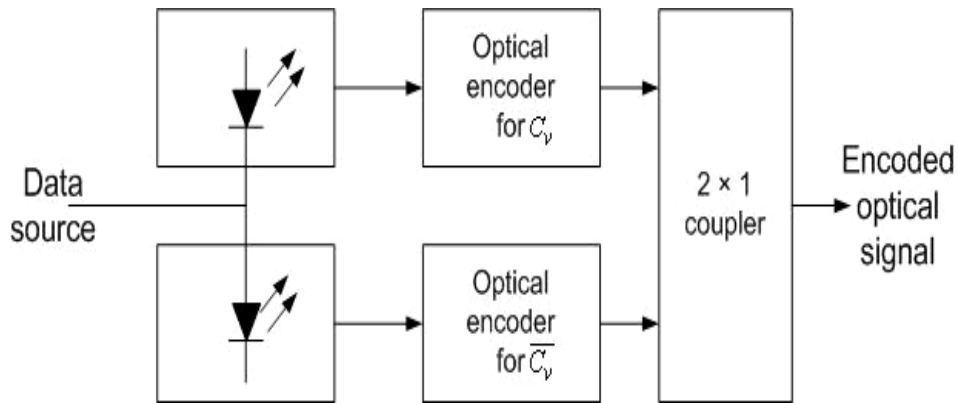
Figure 5-1: Structure of the MCMLC encoder.

Figure 5.2 shows the structure of decoders based on MCMLCs. The received signal is divided into $2^{E+1}v/2$ branches and then delayed to accumulate the marked chips of C_L^j in the optical correlator. Let P_r be the received optical power per chip at the input of correlator, then power at the output of optical correlator can be written as:
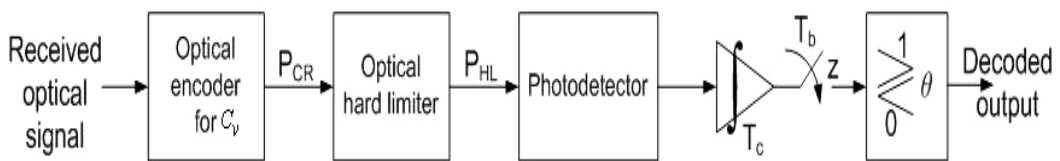

Figure 5-2: MCMLC decoder of the OCDM system.

$$P_{CR} = \begin{cases} P_r\left(\dfrac{L}{2} + I\left(\dfrac{L}{4}\right)\right), & \text{for } b = 1 \\ P_r\left(I\left(\dfrac{L}{4}\right)\right), & \text{for } b = 0 \end{cases} \qquad (5.6)$$

here I is the number of interfering users in the system. Hard limiters have widely been used in optical CDMA systems to reduce the effect of MAI [65-67]. It is an important nonlinear device in all-optical logic processing [68–70]. The bistability of the optical hard limiter can be defined as Equation 5.7:

$$u(x) = \begin{cases} P_{th}, & x \geq P_{th} \\ 0, & 0 \leq x < P_{th} \end{cases} \qquad (5.7)$$

where x is the input optical power and $u(x)$ is the output optical power.

The threshold P_{th} of the hard limiter in Figure 5.2, is set to $P_r L(1 + I)/2$; therefore, the power when data bit 1 is transmitted i.e., $P_r\left(L/2 + I(L/4)\right)$ in Equation (5.6) is clipped to $P_r L(1 + I)/2$ while the power when data bit 0 is transmitted i.e., $P_r(IL/4)$ is clipped to zero. In the next stage, the output of the hard limiter is photodetected. Finally, the integrate-and-dump circuit and the threshold circuit decide whether the received bit is 0 or 1. The optimal threshold θ that minimizes the BER will be further discussed in the next Section.

5.4   Performance Analysis

In this section, the performance of the OCDM system presented above is analysed. The photodetector is assumed to be APD, and the Gaussian model

including APD noise and thermal noise is employed. It is worth mentioning here that though in chapter 3 we have argued that the use of APD does not always results in the optimal performance but still the use of APD in the analysis here is adopted because it makes the analysis more general.

Since the threshold of the hard limiter is set to $(1+I)L/2$; the output power of the hard limiter, denoted P_{HL}; can be expressed as:

$$P_{HL} = \begin{cases} \dfrac{P_r L(1+I)}{2}, & \text{for } b = 1 \\ 0, & \text{for } b = 0 \end{cases} \qquad (5.8)$$

It is assumed that the number of active users is N and that there are I interfering users. Furthermore, without loss of generality, it is assumed that the first user is the desired user and that b_0 is the desired bit. The average photon arrival rate λ per pulse at the input of the optical correlator is given by $\lambda = \eta P / hf$.

According to correlation property of PDC each user contributes one spectral component in the desired user's signal and is given is:

$$I = \sum_{k=1}^{K} i_k \qquad (5.9)$$

Given $N = I$ and the desired bit $b_0 = 1$, using Gaussian expression:

$$P_Y(Y = y \mid b_0 = 1) = \frac{1}{\sqrt{2\pi\sigma_1^2}} \exp\left[-\frac{(y-\mu_1)^2}{2\sigma_1^2}\right] \qquad (5.10)$$

The mean and variance of output Z after the sampler given I and $b_0 = 1$ can be expressed as:

$$\mu_1 = GT_c\left[\frac{L}{2}(1+I)\lambda + \frac{I_b}{e}\right] + \frac{T_c I_s}{e} \tag{5.11}$$

$$\sigma_1^2 = G^2 F_e T_c\left[\frac{L}{2}(1+I)\lambda + \frac{I_b}{e}\right] + \frac{T_c I_s}{e} + \sigma_{th}^2 \tag{5.12}$$

where, G is the average APD gain.

Similarly, given I and $b_0 = 0$,

$$P_Y(Y = y \mid b_0 = 0) = \frac{1}{\sqrt{2\pi\sigma_0^2}}\exp\left[-\frac{(y-\mu_0)^2}{2\sigma_0^2}\right] \tag{5.13}$$

where:

$$\mu_0 = GT_c\frac{I_b}{e} + \frac{T_c I_s}{e} \tag{5.14}$$

$$\sigma_0^2 = G^2 F_e T_c\frac{I_b}{e} + \frac{T_c I_s}{e} + \sigma_{th}^2 \tag{5.15}$$

Assuming that the probability of $b = 1$ is equal to that of $b = 0$; the BER of the proposed OCDM system can be derived as:

$$P_e = \Pr\{b = 0\}\cdot\Pr\{Y \geq \theta \mid b = 0\} + \Pr\{b = 1\}\cdot\Pr\{Y < \theta \mid b = 1\} \tag{5.16}$$

$$P_e = \frac{1}{4}\left\{ erfc\left(\frac{\theta - \mu_0}{\sqrt{2\sigma_0^2}}\right) + erfc\left(\frac{\mu_1 - \theta}{\sqrt{2\sigma_1^2}}\right)\right\} \qquad (5.17)$$

and, $erfc(\cdot)$ stands for the complementary error function is defined as:

$$erfc\,(x) = \frac{2}{\sqrt{\pi}}\int_x^\infty \exp\left(- y^2\right)dy \qquad (5.18)$$

To minimize the BER, the optimal threshold θ can be derived as:

$$\theta = \begin{cases} (\mu_1 + \mu_0)/2, & \text{for } \sigma_1^2 = \sigma_0^2 \\ \dfrac{b + \sqrt{b^2 - ac}}{a}, & \text{for } \sigma_1^2 \neq \sigma_0^2 \end{cases} \qquad (5.19)$$

where

$$a = \sigma_1^2 - \sigma_0^2 \qquad (5.20)$$

$$b = \sigma_1^2 \mu_0 - \sigma_0^2 \mu_1 \qquad (5.21)$$

$$c = -\ln\left(\frac{\sigma_1^2}{\sigma_0^2}\right)\sigma_0^2\sigma_1^2 - \sigma_0^2\mu_1^2 + \sigma_1^2\mu_0^2 \qquad (5.22)$$

5.5   Numerical Results

In this Section, the numerical results are calculated according to the system model presented in Section 5.4 and the parameters listed in Table 4.5. The MCMLC-OCDM system considered in this Section is assumed to be the single rate system.

Figure 5.3 plots the BER of the MCMLC systems against the number of users N. It is interesting to note in the figure that the bit error rate performance is improved as the number of users N in the systems increase. This can be explained by careful look of Equation (5.6), which shows that the difference in P_{HL} between bits 1 and 0 increases as N increases. However, it should be noted that in the analysis presented for MCMLCs in section 5.4 Gaussian model is used and ignores the effect of phase-induced intensity noise, which is the major factor of noise contribution in any optical communication system. Therefore, this behavior depicted in Figure 4.3 can be changed when PIIN is incorporated in the system as PIIN is directly propotional to the number of users in the system.

In most of the spectral amplitude coding systems in the literature using OOK as modulation technique and Modified Prime codes or PDCs as signature sequences, even though the total number of users N that can be accommodated is kept fixed it provides only a little information about the MAI power at any instant since the number of users who are sending bit 1s varies randomly. Consequently, the performances of the MPC without hard limiters and PDC systems without interference estimators are much poorer than the performance of the MCWC system. As in the case of MCWC no matter users in the system transmit data bit 1 or 0, a code is always transmitted which contributes a fixed level of interference in the desired user's signal. Hence, eliminating the interference from information signal is easier. By inspecting the curves in Figure 4.3, it is obvious that the BER of the proposed MCMLC systems with lower received power ($P_r = -70$ dBW, -75 dBW, -80 dBW) is much smaller as long as N is large enough.
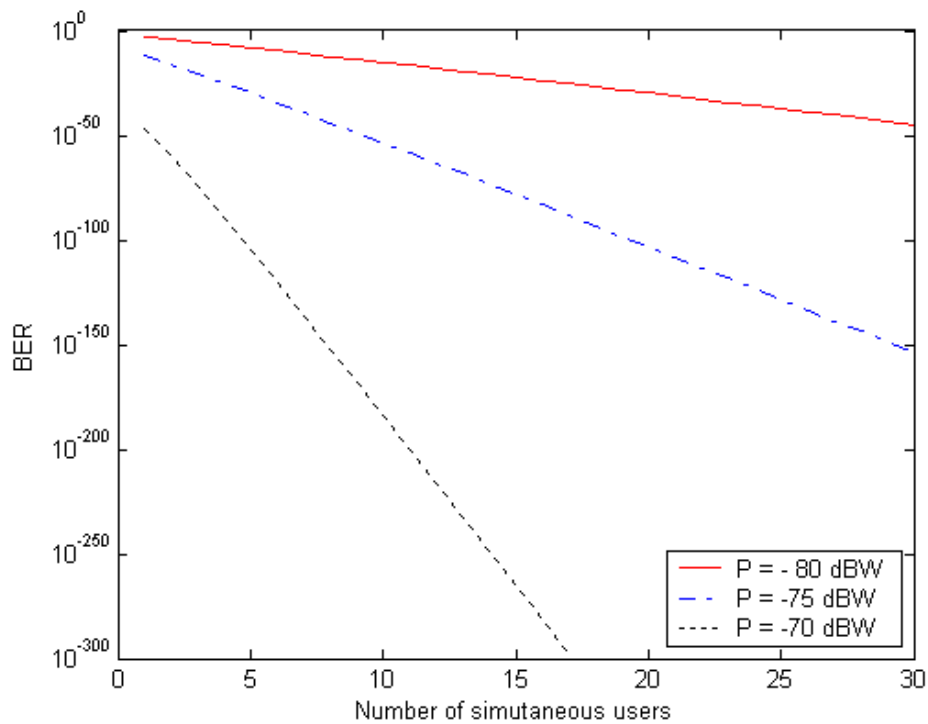
Figure 5-3: BER versus number of users for MCMLCs and w = 4.

Confirming the response of the system illustrated in Figure 5.3, Figure 5.4 shows the relation between the number of simultaneous users and the SNR for both MCMLCS and MCMWs with similar length 16 and weight of 4 and received power of – 70 dBW. It has been shown that MCML code gives a much higher SNR than MCWC.
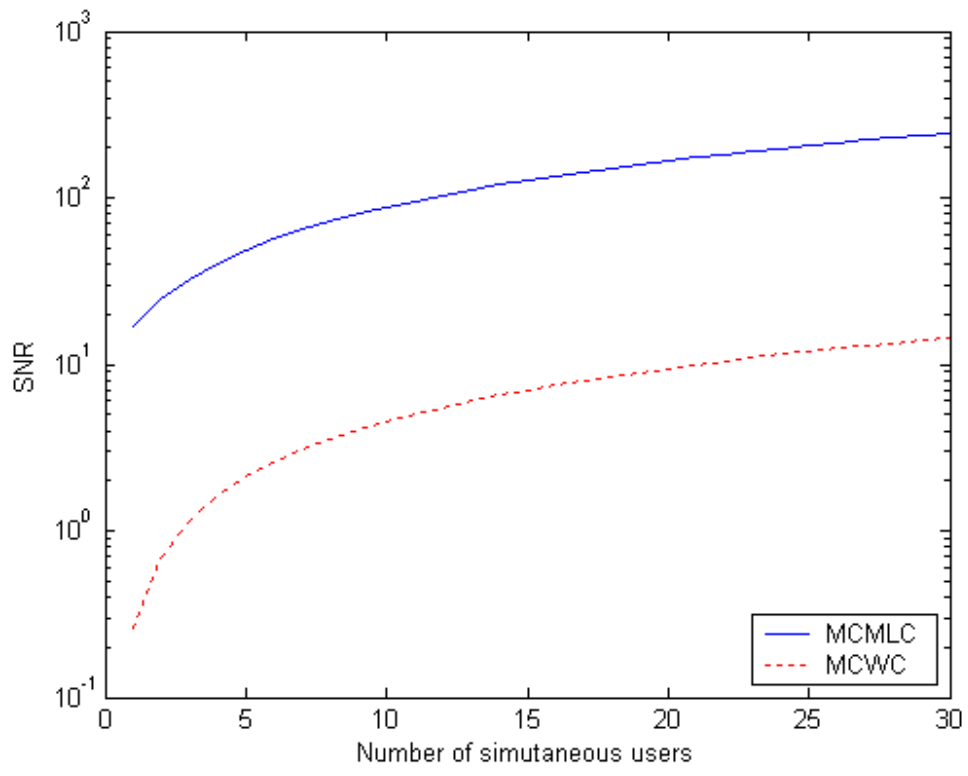
Figure 5-4: SNR versus number of users for MCMLCs for P = – 70 dBW and w = 4.
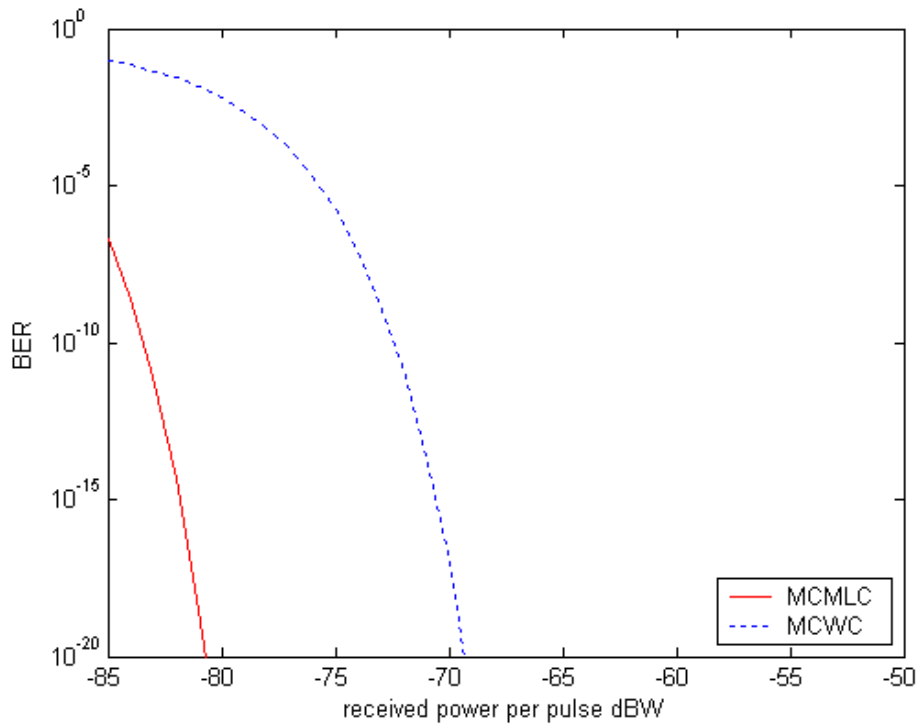
Figure 5-5: BER versus received power per pulse under full load for MCMLC and MCWC.

Figure 5.5 shows the fully loaded BER curve against the received power per chip P_r of the MCMLC systems together with the same for the MCWC systems. The superiority of the MCWC system is again apparent in Figure 5.5. For example, to achieve BER of $\leq 10^{-09}$; MCWC system needs a receive power P_r of -73 dBW while the MCMLC needs only only -80 dBW.

5.6   Summary

The new family of spreading sequences namely Manchester-coded Modified Legendre sequences are presented in this chapter. The bit error rate performance of the OCDM system utilizing MCMLCs is also analyzed. The proposed sequences are suitable to be used with both single rate and multirate systems.

6. Application of Perfect Difference Codes in Wireless Infrared Systems

In this chapter, the perfect difference codes are applied in wireless infrared systems and analyze the bit error rate performance of the system using Gaussian approximations.

6.1 Introduction

The past few decades have seen the increased interest of the researchers in the utilization of infrared (IR) frequencies for short range wireless communications [71-75]. Wireless radio technologies have been designed and implemented comparatively over a much longer time than wireless infrared systems, however, the low complexity and low cost of infrared systems make relatively new IR systems very attractive and cost effective solution at a bit rates up to several tens of Mbps. Many potential applications for this technology, such as Wireless LANs, have already been suggested.

As briefly discussed in chapter 2, the diffuse indoor optical wireless configuration (i.e. non-directed, non-line of sight) is one of the most convenient and robust one

for local area networks (LAN). In the diffuse configuration, the transmitters and the receivers of infrared systems do not require to be carefully aligned, nor do they need to be in a line-of-sight (LOS) path so that communication can be maintained. The other major advantages of diffuse systems are their flexibility and the roaming they allow in a room. This flexibility makes them the ideal choice for ad hoc networks and gives the end users freedom to roam freely insider the office or room. In this chapter, therefore, a diffuse configuration is considered. However, this freedom of roaming results in the problems associated with high path loss and inter-symbol interference (ISI) due to multipath dispersion. In a code-division based WIR systems, the effects of ISI can be compensated by using efficient spreading sequences.

In this chapter, the perfect difference codes are applied for the first time in indoor optical wireless channel. A wireless infrared system is proposed which uses the encoders/decoders as explained in chapter 5. The performance analysis of such system is analyzed in terms of bit error rate versus path loss and bit error rate versus number of users.

6.2   System model

The number of active users is $I+1$ and $N_{\max}$ is maximum allowed number of users which can be associated to each station. We use PDC based OCDMA as uplink multiple access technique. The average received power using PDC is expressed by [76]

$$P_r = \frac{w}{2v} I_r A_d \qquad\qquad (6.1)$$

where I_r = is the received light intensity

A_d = is the area of photodetector.

6.2.1 Channel Model

One of the most important parameters that affect the performance of infrared system is the channel path loss which is the DC-gain (H_0) of the channel transfer function. It can be expressed as:

$$P_r = H_0 P_t \qquad\qquad (6.2)$$

relating the transmitted (P_t) and received (P_r) average powers.

Figure 6.1 illustrates the non-directed non-line of sight configuration selected for the system under study in which the transmitter and receiver are pointed straight upward and transmitter emits a Lambertian pattern. The h_1 and h_2 represents the distance of transmitter and receiver from the ceiling, with diffuse reflectivity ρ, respectively. We assume that the diffuse reflectivity of ceiling is 80%. The path loss for diffuse link is plotted in Figure 6.2 which is measured in any typical office [74].
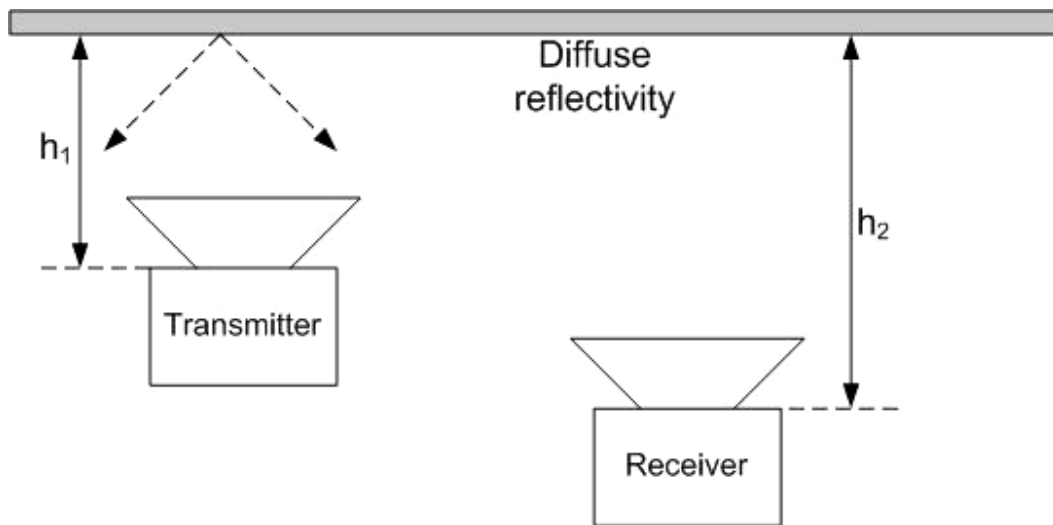
**Figure 6-1:** Non-directed non-line of sight LOS (Diffuse) configuration.
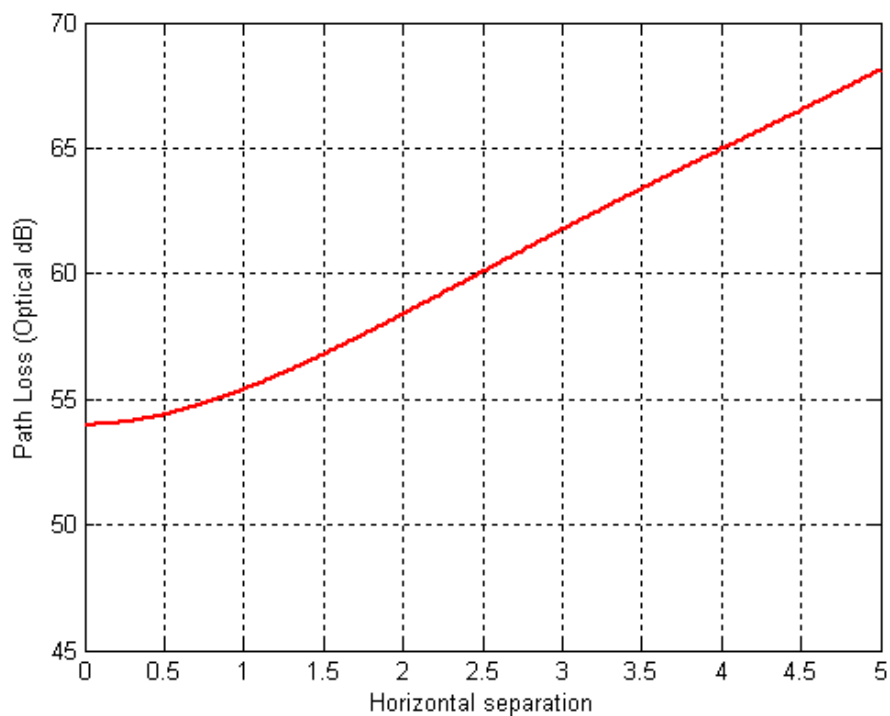
Figure 6-2: Optical path loss of a diffuse infrared links employing a Lambertian transmitter and a detector of area $A_d = 1$ cm^2 and reflectivity of 80% measured in a typical room.

6.2.2 Transmitter & Receiver

At the transmitter on-off keying intensity modulation scheme is adopted and direct detection at the receiver. Duration of each chip is $T_c = T_b / v$ where v is the code length and T_b is the bit duration. At the receiver, a composite signal containing the desired signal along with the noise and interference from all other I active users passed through the channel is detected. The receiver's structure is assumed to be similar to one as illustrated in Figure 5.2 that is based on correlation detection. At the receiver all the weighted chips of the desired sequence are summed to form a decision variable. This decision variable is compared to a threshold to detect data bit 1 or 0 [77].

6.3 Performance Analysis

In this analysis, it is assumed that different nodes transmit asynchronously and independently. Further to make things simpler, different signals are assumed to be chip synchronous, which is a pessimistic case and gives an upper bound to the BER of the real asynchronous system [77].

The number of interfering pulses received in j_{th} pulse position of the desired codeword is denoted by $\phi_j = 1, 2, \ldots, K$. The vector of received interference is

denoted by $\vec{\phi} = (\phi_1, \phi_2, \ldots, \phi_K)$. In light of the cross-correlation property of PDC, two code-words cannot overlap at more than one pulse position. Therefore, the probability that two codewords overlap at one pulse position is $q = w^2 / 2v$ where factor 1/2 accounts for the probability that interfering user sent "one" only half time.

Given I interfering users, the BER of the desired user's signal can be expressed as [78]:

$$P_e = \sum_{i=0}^{I} P_r(i) P(F_i) \tag{6.3}$$

where $P_r(i)$ is the probability that there are l interfering pulses, which is given by:

$$P_r(i) = \binom{I}{i} q^i (1-q)^{I-i} \tag{6.4}$$

F_i is the set of all possible $\vec{\phi}$ vectors. Since the l interfering users are not distinguishable in correlation receiver, $P(F_i) = P(\vec{\phi})$.

Using Gaussian approximation for photon detection, $P(\vec{\phi})$ can be written as [78]:

$$P(\vec{\phi}) = 0.5Q\left(\frac{\theta - \mu_0}{\sqrt{\sigma_0}}\right) + 0.5Q\left(\frac{\mu_1 - \theta}{\sqrt{\sigma_1}}\right) \tag{6.5}$$

where

$$Q(x) = \frac{1}{\sqrt{2\pi}} \int_x^{\infty} e^{-\frac{y^2}{2}} \, dy \qquad (6.6)$$

Let P_r be the received optical power per chip at the input of correlator, then power at the output of optical correlator can be written as

$$P_{CR} = \begin{cases} P_r(w + I), & \text{for } b = 1 \\ P_r(I), & \text{for } b = 0 \end{cases} \qquad (6.7)$$

here w is the weight of the PDC, I is the number of interfering users in the system.

The threshold P_{th} of the hard limiter is set to $P_r(w + 2I)/2$; therefore, the power $P_r(w + I)$ in Equation (6.7) is clipped to $P_r(w + 2I)/2$ while the power $P_r(I)$ is clipped to zero. After that, the output of the hard limiter is transformed to an electronic signal by the photodetector. Finally, the integrate-and-dump circuit and the threshold circuit decide whether the received bit is 0 or 1.

The average photon arrival rate λ per pulse at the input of the optical correlator is given by $\lambda = \eta P_r / hf$. According to correlation property of PDC each user contributes one spectral component in the desired user's signal and the mean photon count produced by the i_{th} interferer, which is a function of ρ_i (path loss) and transmission power, is given is:

$$I(\rho) = \sum_{k=1}^{K} i_k, \qquad (k = 1,2,\ldots N\text{-}1) \qquad (6.8)$$

Given $N = I$ and the desired bit $b_0 = 1$, using Gaussian expression:

$$P_Y(Y = y \mid b_0 = 1) = \frac{1}{\sqrt{2\pi\sigma_1^2}} \exp\left[-\frac{(y-\mu_1)^2}{2\sigma_1^2}\right] \qquad (6.9)$$

The mean and variance can be expressed as:

$$\mu_1 = GT_c\left(\frac{(k+2I)\lambda}{R_b} + \frac{kI_d}{e}\right) + GT_c\left(\frac{\eta A_d m_b}{hf}\right) \qquad (6.10)$$

$$\sigma_1^2 = G_1^2 F_{e1} T_c\left[\frac{(k+2I)\lambda}{R_b} + \frac{kI_d}{e}\right] + GT_c\left(\frac{\eta A_d m_b}{hf}\right) + \sigma_{th}^2 \qquad (6.11)$$

where A_d is the photodetector's area, m_b is the mean photon count of the ambient light noise, and I_d is the dark current.

Given $N = I$ and the desired bit $b_0 = 0$, using Gaussian expression, the mean and variance can be expressed as:

$$\mu_0 = GT_c\left(\frac{kI_d}{e}\right) + GT_c\left(\frac{\eta A_d m_b}{hf}\right) \qquad (6.12)$$

$$\sigma_0^2 = GT_c\left[\frac{kI_d}{e}\right] + GT_c\left(\frac{\eta A_d m_b}{hf}\right) + \sigma_{th}^2 \qquad (6.13)$$

To minimize the BER, the optimal threshold θ can be derived as:

$$\theta = \begin{cases} (\mu_1 + \mu_0)/2, & \text{for } \sigma_1^2 = \sigma_0^2 \\ \dfrac{b + \sqrt{b^2 - ac}}{a}, & \text{for } \sigma_1^2 \neq \sigma_0^2 \end{cases} \qquad (6.14)$$

where

$$a = \sigma_1^2 - \sigma_0^2 \qquad (6.15)$$

$$b = \sigma_1^2 \mu_0 - \sigma_0^2 \mu_1 \qquad (6.16)$$

$$c = -\ln\left(\frac{\sigma_1^2}{\sigma_0^2}\right)\sigma_0^2\sigma_1^2 - \sigma_0^2\mu_1^2 + \sigma_1^2\mu_0^2 \qquad (6.17)$$

6.4　Numerical Results

In this part some numerical results are presented for the wireless infrared system discussed above. The infrared CDMA system is assumed with data rate of $R_b = 2$ Mbps per user and PDC codewords with length $v = 183$ and weight $w = 14$. The system is operating at the wavelength of $\lambda = 850$ nm, the ambient light noise intensity is $m_b = 490 \, \mu\text{W/cm}^2$ the quantum efficiency of the photodetector is $\eta = 0.6$, photodetector's area is $A_d = 1 \, \text{cm}^2$ and dark current is assumed to be $I_d = 160$ nA.
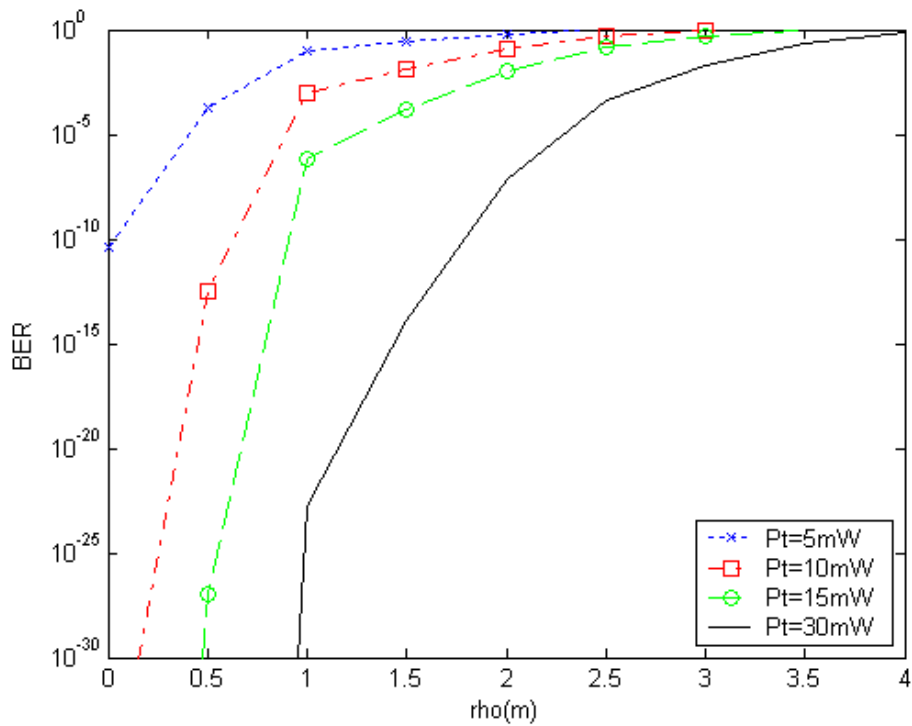
Figure 6-3: BER versus user's difference from base station (ρ) for various transmission powers. Number of interferes is 5.

Figure 6.3 illustrates the bit error rate performance of the indoor optical distance versus the user's distance (ρ) from the base station for transmission powers of 5 mW, 20 mW, 15 mW and 30 mW. The number of interfering users is kept fixed. One can see the near-far problem in a basic PDC wireless infrared network without power control. As the distance from the base station is increased the system performance degrades rapidly. This shows that the users which are near the base station obtain much more BER than needed but the data from far users can not be detected with desired BER. This generates the requirement of a power control algorithm in indoor wireless system to make sure that all users regardless

of their distance from the base station can access the base station with equal power.
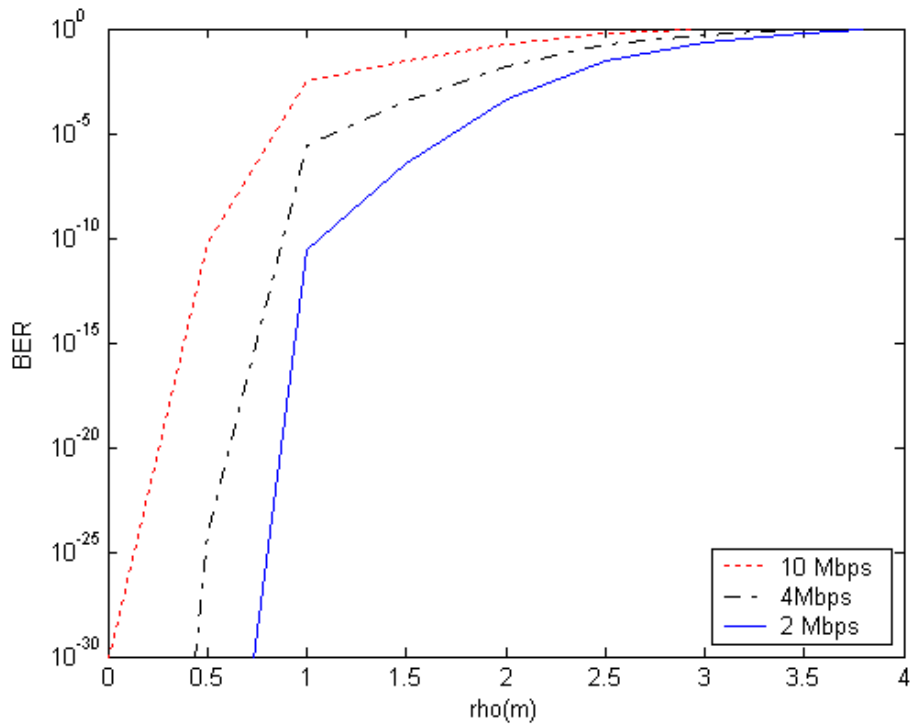
Figure 6-4: BER versus user's distance from base station (ρ) for various bit rates. Number of interferes is 5 and Pt = 20 mW.

Figure 6.4 plots the error probability versus user's distance from the base station for different bit rates (2, 4 and 10 Mbps). The transmitted power and the number of interferes is kept fixed at P_t = 20 mW and 5, respectively. It can be seen that the path loss as the user's move away from the base station puts severe restrictions on the data rate. In Figure 6.5, the bit error rate versus number of users

is plotted. Similar to the curves obtained in chapter 5 it can be seen here that as the number of users increase the bit error rate performance is improved. The reason for this again can be found in Equation (6.7) which shows the increase in the number of users is directly proportional to the difference between data bit 1 and 0.
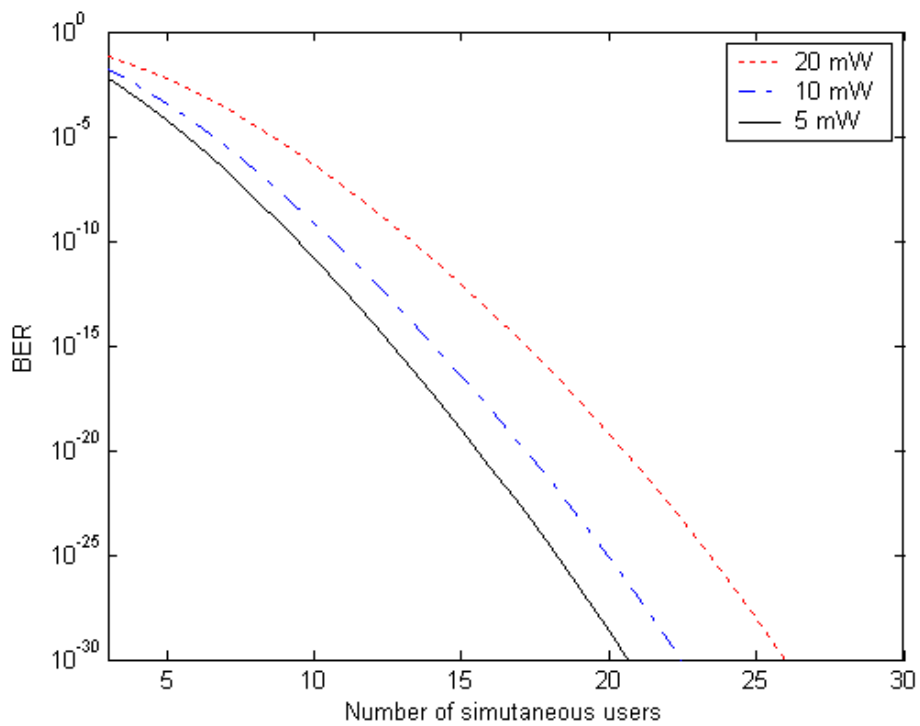
Figure 6-5: Error probability versus number of users for data rate of 2 Mbps.

6.5   Summary

In this chapter, perfect difference codes are applied in wireless domain. The uplink performance in presence of various noise sources such as path loss, ambient noise, multiple access interference and thermal noise is analyzed. The bit error rate performance was analyzed over different transmission powers and different data rates. It is revealed from the results that an effective power control algorithm is required to mitigate path loss effects.

7. Conclusions and Future work

7.1 Conclusions

In this chapter conclusions will be made and also some recommendations for future work will be given.

The thesis addressed the challenges of mitigating MAI effect, designing efficient encoders/decoders, and the design of codes that can support Multirate services posed by optical communication networks.

The thesis begins by presenting the motivation and objectives of the work in the first chapter. Perfect difference codes are focused in this work due to their interesting properties and applied in both wired and wireless optical communication systems.

A novel and simple encoding and decoding architecture is proposed utilizing common zero code technique for optical code division multiplexing systems with the capabilities of effectively reducing MAI without complex decoding circuitry and detecting algorithms. The performance of PDCs structured on the proposed encoder/decoders is analyzed using Gaussian model ignoring PIIN and also analytical expression of SNR is derived considering PIIN in terms of bit error

rate, signal-to-noise ratio, and power constraints. The analytical results show that the proposed architecture is able to provide MAI free operation for CDMA systems.

A new family of spreading sequences called Manchester coded modified-Legendre sequences is designed. The proposed spreading sequences are suitable to meet the multi-traffic demands of future networks. The performance of MCMLCs is analyzed using Gaussian model in terms of bit error rate and signal to noise ration. The analytical results show the superior performance to other conventionally used spreading sequences.

Perfect difference codes for the first time were applied in indoor optical wireless communication system. The uplink performance in terms of bit error rate, path loss and number of users was analyzed. The results revealed that an effective power control algorithm is required to mitigate path loss effects.

7.2   Future Directions

Finally, some directions for future work are presented below:

- The performance analysis of the spectral amplitude coding systems based OCDMA system presented in this thesis focuses its attention on the physical layer effects such as, multiple access interference, phase-induced intensity noise, ambient noise, thermal noise, surface leakage current, dark current, APD gain mismatch and other photo detector impairments. In particular it is imperative that further study should be given to the effects

111

of interfacing physical layer with higher network layers; and on the development of photonic devices which will facilitate cost-effective OCDMA deployment. There is also a compelling need in applying error correction codes in order to increase effective throughput. It remains to be explored in which network layer error correcting codes should be deployed, and in particular whether multiple access coding and error correction coding may fruitfully be integrated.

- In chapter 6, the results show that in indoor optical wireless system the user's that are located far from the base station cannot maintain the same bit error rate as compared to those which are nearer the bases station. This problem can be solved by employing Power control algorithms in infrared systems. To investigate the impact of using power control techniques in wireless infrared system is the interesting topic awaiting further research.

- Since UWB is an emerging technology with many unique properties, it is offering considerable research potential. Owing to the ultra narrow pulse of UWB, synchronization is the most challenging task in the UWB receiver. The channel matched filter would operate at extremely high sampling rates and a coherent RAKE would consist of a large number of correlator arms making the decoding complicated and unaffordable. Therefore, the non-coherent receivers become attractive candidates for low complexity and low-power IR-UWB systems. The spreading sequences tailor-made for incoherent communication system such as

perfect difference codes can be interesting topic to explore in radio domain.

References

[1]   Andrew Stok and Edward H. Sargent, "Lighting the Local Area: Optical Code-Division Multiple Access and Quality of Service Provisioning," IEEE Network, November/December 2000.

[2]   Pruncal P. R, M. A. Santro, and T. R. Fan, "Spread Spectrum Fiber – Optic Local Area Network using Optical Processing," Journal of Lightwave Technology, Vol. 4, pp. 547 – 554, 1986.

[3]   J. A. Salehi, "Code division multiple-access techniques in optical fiber networks - part I: Fundamental principles," IEEE Transactions on Communications, Vol. 37, pp. 824-833, 1989.

[4]   Xhi-Shun Weng; Jingshown Wu; "Perfect difference codes for synchronous fiber-optic CDMA communication systems", Journal of Lightwave Technology, Vol. 19, pp. 186 – 194, 2001.

[5]   J. S. Jhou1, J. Y. Lin, and J. H. Wen, "Performance enhancement of perfect difference codes with spectral amplitude coding using sub-optimal decision threshold," European Transactions On Telecommunications, Vol. 18, pp. 745 – 759, 2007.

[6]   Kochevar H. J, "Spread Spectrum Multiple Access Communication Experiment through a Satellite," IEEE Transactions on Communications, Vol. 27, pp. 853 – 856, 1979.

[7]   Pickholtz R. L, D. L. Schilling, and L. B. Milstein, "Theory of Spread-Spectrum Communications - A Tutorial," IEEE Transactions on Communications, Vol. 30, pp. 855 – 884, 1982.

[8]   Dixon R. C, Spread Spectrum Systems, 2nd Edition, New York: John Wiley & Sons, 1984.

[9]   Pursely M. B, Spread Spectrum Multiple-Access Communications in Multi-user Communication Systems, G. Longo (ed.), New York: Spring-Verlag, 1981.

[10]   M. J. Parham, C. Smythe and B. L. Weiss, "Code division multiple access techniques for use in optical-fiber local-area networks", Electronics & Communication Engineering Journal, pp. 202 – 212, 1992.

[11]   Kleinrock L and F. A. Tobagi, "Packet Switching in Radio Channels: Part I – Carrier Sense Multiple-Access Modes and their Throughput-Delay Characteristics," IEEETransactions on Communications, Vol. 23, pp. 1400 – 1416, 1995.

[12] Vannucci, G and S. Yang, "Experimental Spreading and Despreading of the Optical Spectrum," IEEE Transactions on Communications, Vol. 37, pp. 770 – 780, 1989.

[13] Salehi, B. E. A, and M. C. Teich, Fundamentals of Photonics, New York: John Wiley & Sons, 1991.

[14] Blahut R. E, Theory and Practice of Error Control Codes, Reading, MA: Addison Wesley, 1984.

[15] Shaar, A. A., and P. A. Davies, "Prime Sequences: Quasi-Optical Sequences for OR Channel Code Division Multiplexing," Electronics Letters, Vol. 19, pp. 888 – 890, 1983.

[16] Tamura S, S. Nakano, and K. Okazaki, "Optical Code-Multiplex Transmission by Gold Sequences," Journal of Lightwave Technology, Vol. 3, pp. 121 – 127, 1985.

[17] A. M. Weinet and j. A. Salehi, "Optical code-division multiple-access," Photonics in Switching (J. E. Midwinter, ed) San Diego, CA: Academic Press, Vol. 2, pp. 73 – 118, 1993.

[18] B. Mukherjee, Optical Communication Networks, New York: McGraaw-Hill, 1997.

[19] Miller, S. E, and I. P. Kaminow (eds.), Optical Fiber Telecommunications II, Los Angeles: Academic Press, 1988.

[20] M. Nakazawa, E. Yoshida, T. Yamamoto, E. Yamada, and A. Sahara, "TDM single channel 640 Gbps Transmission Experiment over 60 km using 400fs Pulse Train and Walk-Off Free, Dispersion Flattened Nonlinear Optical Loop Mirror," Electronics Letters, Vol. 34, pp. 907 – 908, 1998.

[21] Silvia Diaz, Gorka Lasheras, and Manuel Lopez-Amo, "WDM bi-directional transmission over 35 km amplified fiber-optic bus network using Raman amplification for optical sensors", Optics Express, Vol. 13, pp. 9666-9671, 2005.

[22] Jackson, K. P., et al., "Optical Fiber Delay-Line Signal Processing,," IEEE Transactions on Microwave Theory and Techniques, Vol. 33, pp. 193 – 210, 1985.

[23] Molsehi, B., et al., "Fiber-Optics Lattice Signal Processing" Proc. of the IEEE, Vol. 72, pp. 909 – 930, 1984.

[24] Chung, F. R. K, J. A. Salehi, and V. K. Wei, "Optical Orthogonal Codes: Design, Analysis and Applications," IEEE Transactions on Information Theory, Vol. 35, pp. 595 – 604, 1989.

[25] Gfeller FR, and Bapst U, "Wireless in-house data communications via diffused infrared radiation," Proceedings of the IEEE, Vol. 67, pp. 1474 – 1486, 1979.

[26]   Barry JR, Wireless Infrared Communications, Kluwer Academic Publishers: Dordrecht, 1994.

[27]   Z. Ghassemlooys and A. R. Hayes, "Digital pulse interval modulation for IR communication systems – a review," International Journal Of Communication Systems, Vol. 13, pp. 519 – 536, 2000.

[28]   R. J. Dickensonz and Z. Ghassemlooy, "Wavelet–AI equalization and detection for indoor diffuse infrared wireless systems," International Journal of Communication Systems, Vol. 18, 247–266, 2005.

[29]   Steve Hranilovic, "On the Design of Bandwidth Efficient Signalling for Indoor Wireless Optical Channels," International Journal of Communication Systems, Vol. 18, pp. 205–228, 2005.

[30]   Yun G, Kavehrad M, "Spot Diffusing and fly-eye receivers for indoor infrared wireless communications," Proceedings of the 1992 IEEE Conference on Selected Topics in Wireless Communications, Vancouver, Canada, 286–292, 1992.

[31]   Akhavan K, Kavehrad M, Jivkova S, "Wireless infrared in-house communications: how to achieve very high bit rates," WCNC 2000-IEEE Wireless Communications and Networking Conference, Vol. 1, pp. 698–703, 2000.

[32]   Jivkova S, Kavehrad M, "Receiver designs and channel characterization for multi-spot high-bit-rate wireless infrared communications," IEEE Transactions on Communications, Vol. 49, pp. 2145–2153, 2001.

[33]   Gene W. Marsh, and Joseph M. Kahn, "Channel Reuse Strategies for Indoor Infrared Wireless Communications," IEEE Transactions on Communications, Vol. 45, October 1997.

[34]   A. Mendez, R. Gagliardi,H. Feng, J. Heritage,and J. Morookian, "Strategies for Realizing Optical CDMA for Dense, High-Speed, Long Span, Optical Network Applications," Journal of Lightwave Technology, Vol. 18, 2000.

[35]   K. K. Wong, T.O'Farrell and M. Kiatweerasakul, "Infrared Wireless Communication using Spread Spectrum Techniques", IEE Proc. Optoelectron., Vol. 147, No. 4, 2000.

[36]   L. Tancevski, I. Andonovic, M. Tur, J. Budin, "Massive Optical LANs Using Wavelength Hopping/Time Spreading with Increased Security", IEEE Photon. Technology Letters, Vol. 8, pp. 935 – 937, 1996.

[37]   K. K. Wong, "Bandwidth Efficient Modulation Techniques for Spread Spectrum Bared Wireless Infrared Transmission," Ph.D. thesis, Univ. of Leeds. U.K., 2002.

[38] K. K. Wong and T. O'Farrell, "Biarthoganal Direct- Sequence Spread Spectrum System for Infrared Wireless Communications," 77th IEEEPIMRC. London. U.K., pp. 933-38, 2000.

[39] J. A. Salehi, A. M. Weiner, and J. P. Heritage, "Coherent Ultrashort Light Pulse CDMA Communication Systems," J. Lightwave Technol. Vol. 8, pp. 478–491, 1990.

[40] Z. Jiang, D. Seo, S. Yang, D. E. Leaird, R. V. Roussev, C. Langrock, M. M. Fejer, and A. M. Weiner, "Four-user 10-Gb/s spectrally phase-coded O-CDMA system operating at 30 fJ/bit," IEEE Photon. Technol. Lett., Vol. 17, pp. 705–707, 2005.

[41] D. Zaccarin and M. Kavehrad, "An optical CDMA system based on spectral encoding of LED," IEEE Photon Technology Letters. Vol. 04, pp. 479 – 482, 1993.

[42] M. Kavehrad and D. Zaccarin, "Optical code-division-multiplexed systems based on spectral encoding of noncoherent sources", J. Lightwave Technology, Vol. 13, pp. 534–545, 1995.

[43] L. Nguyen, B. Aazhang, and J. F. Young, "All-optical CDMA with bipolar codes", Electronics Letters, Vol. 31, pp. 469–470, 1995.

[44] C. F. Lam, D. K. Tong, M. C.Wu, and E. Yablonovitch, "Experimental demonstration of bipolar optical CDMA system using a balanced

transmitter and complementary spectral encoding," IEEE Photonic Technology Letters, Vol. 10, pp. 1504–1506, 1998.

[45]   E. D. J. Smith, P. T. Gough, and D. P. Taylor, "Noise limits of optical spectral-encoding CDMA systems," Electronics Letters, Vol. 31, pp. 1469–1470, 1995.

[46]   X. Wang and K. Kitayama, "Analysis of beat noise in coherent and incoherent time-spreading OCDMA," Journal of Lightwave Technology, Vol. 22, 2005, 2226–2232 Optical Society of America JON 7657, Vol. 4, Journal of Optical Networking 630, 2005.

[47]   E. D. J. Smith, R. J. Blaikie, and D. P. Taylor, "Performance Enhancement of Spectral-Amplitude Coding optical CDMA using Pulse-Position Modulation," IEEE Transactions on Communications. Vol. 46, pp. 1176–1185, 1998.

[49]   Y. Maeda, K. Okada, and D. Faulkner, "FSAN OAN-WG and future issues for Broadband Optical Access Networks," IEEE Commununications Magzine, Vol. 12, pp. 126–132, 2001.

[50]   A, T. Pham, N. Miki, H. Yashima, "Spectral-Amplitude-Encoding Optical-Code-Division-Multiplexing System with a Heterodyne Detection Receiver for Broadband Optical Multiple-Access Networks," Journal of Optical Networking, Vol. 4, pp. 621 – 631, 2005.

[51]   G. P. Agrawal, Fiber-Optic Communication Systems, 2nd ed., Wiley-Inter science, 1997.

[52]   Z. Wei, H. M. H. Shalaby, and H. Ghafouri-Shiraz, "Modified Quadratic congruence codes for Fiber Bragg-Grating-based Spectral-Amplitude-Coding optical CDMA Systems," Journal of Lightwave Technology, Vol. 19, pp. 1274–1281, 2001.

[53].   Hossam M. H. Shalaby, "Synchronous Fibre-Optic CDMA Systems with Interference Estimators", IEEE J. of Lightwave Technology, Vol. 17, pp. 2268 – 2275, 1999.

[54]   Kwon, H.M.; "Optical orthogonal code-division multiple-access system .I. APD noise and thermal noise" Communications, IEEE Transactions on Vol. 42, pp. 2470 – 2479, 1994.

[55]   Takahashi H, Oda K, Toba H, Inoue Y, "Transmission characteristics of arrayed waveguide wavelength multiplexer," IEEE Journal of Lightwave Technology, Vol. 13, pp. 447–455, 1995.

[56]   [URL: http://www.fdk.co.jp/whatsnew-e/release040913-e.html]   last accessed June 2008.

[57]   Wei Z, Ghafouri-Shiraz H. "Codes for Spectral-Amplitude-Coding Optical CDMA Systems", IEEE Journal of Lightwave Technolog, Vol. 20, pp. 284-1291, 2002.

[58] Djordjevic IB,Vasic B. "Unipolar codes for spectral-amplitude-coding optical CDMA systems based on projective geometries", IEEE Photonics Technology Letters, Vol. 15, pp. 1318-1320, 2003.

[59] Chao-Chin Yang, "Modified Legendre sequences for optical CDMA-based passive optical networks", IEEE Communications Letters, Vol. 10, pp. 393 – 395, 2006.

[60] T. Shin-Pin, and J. Wu, "Extended Perfect Difference Codes for SAC Optical CDMA PONs", IEEE Communication Letters, Vol. 12, No. 8, 2008.

[61] Liang-Lin Jau and Yang-Han Lee, "Optical Code-Division Multiplexing Systems using Common-Zero Codes", Microwave and Optical Technology Letters / Vol. 39, No. 2, 2003.

[62] Jen-Fa Huang, Chao-Chin Yang, Shin-Pin Tseng, "Complementary Walsh–Hadamard coded optical CDMA coder/decoders structured over arrayed-waveguide grating routers", Optics Communications Vol. 229, pp. 241–248, 2004.

[63] J. W. Goodman, Statistical Optics. New York: Wiley, 1985.

[64] Jau, L.-L.; Lee, Y.-H., "Optical code-division multiplexing systems using Manchester coded Walsh codes", IEE Proceedings Optoelectronics, Vol. 151, pp. 81 – 86, 2004.

[65]   Wu, J.H., and Wu, J.: 'Synchronous fiber-optic CDMA using hardlimiter and BCH codes', J. Lightwave Technol., Vol. 13, pp. 1169–1176, 1995.

[66]   8 Ohtsuki, T., Sato, K., Sasase, I., and Mori, S.: 'Direct-detection optical synchronous CDMA systems with double optical hard-limiters using modified prime sequence codes', J. Sel. Areas Commun., Vol. 14, pp. 1879–1887, 1996.

[67]   Lin, C.L., and Wu, J.: 'Channel interference reduction using random Manchester codes for both synchronous and asynchronous fiber-optic CDMA systems', J. Lightwave Technol., Vol. 18, pp. 26–33, 2000.

[68]   Sawchuk, A.A., and Strand, T.C.: 'Digital optical computing', Proc. IEEE, Vol. 72, pp. 758–779, 1984.

[69]   14 Brzozowski, L., and Sargent, E.H.: 'Optical signal processing using nonlinear distributed feedback structures', IEEE J. Quantum Electron., Vol. 36, pp. 550–555, 2000.

[70]   Brzozowski, L., and Sargent, E.H.: 'All-optical analog-to-digital converters, hard-limiters, and logic gates', J. Lightwave Technol., Vol. 19, pp. 114–119, 2001.

[71]   F. R. Gfeller, and U. Bapst, "Wireless in-house data communication via diffuse infrared radiation," Proceedings of IEEE., Vol. 67, pp. 1474–1485, 1979.

[72]   Barry, J.R. and J.M. Kahn, "Simulation of multipath impulse response for indoor wireless optical channels", IEEE J. Sel. Area Commun. Vol. 1, pp. 367 - 379, 1993.

[73]   J. B. Carruthers and J. M. Kahn, "Modelling of non- directed wireless infrared channels," IEEE Transa- ction on Communication, Vol. 45, pp. 1260–1268, 1997.

[74]   Kahn, J.M., R. You, P. Djahani, A.G. Weisbin, K.T. Beh, and A.P. Tang. IEEE Commun. Mag. 36 (12) pp. 88, 1998.

[75]   Ghassemlooy, Z. and A. C. Boucouvalas. Intern. J. Communs. Syst. Vol. 18, pp.191, 2005.

[76]   S. Zahedi, J. A. Salehi, M. Nasiri-Kenari, "A Photon Counting Approach to the Performance Analysis of Indoors Wireless Infrared CDMA Networks," Proceedings of IEEE PIMRC'00 London, UK, Vol. 2, pp. 928-932, 2000.

[77]   J. A. Salehi and C. A. Brackett, "Code Division Multiple Access Techniques in Optical Fiber Networks - Part II: Systems Performance Analysis," IEEE Trans. Commun., Vol. 37, pp. 834-842, 1989.

[78]   M. Azizoglu, J. A. Salehi, and Y. Li, "Optical CDMA via Temporal Codes," IEEE Trans. Commun., Vol. 40, pp. 1162–1170, Jul. 1992.

[79] Synchronous optical networking: Wikipedia [URL: http://en.wikipedia.org/wiki/Synchronous_optical_networking] last accessed on January 18, 2010.

[80] [URL: http://www.ripe.net/ripe/meetings/ripe-39/presentations/ripe39-eix/sld010.html] last accessed on January 18, 2010.

[81] M. Hall Jr., *Combinatorial Theory*. London, U.K.: Blaisdell, 1967.

[82] H. J. Ryser, *Combinatorial Mathematics*. New York: Wiley, 1963.

[83] Fahim Aziz Umrani, T. O'Farrell, and Abdul Waheed, "Performance Analysis of PDC-OCDMA System with APD Mismatch", Communications in Computer and Information Science Springer-Verlag, pp 306 – 313, Vol. 20.

Author's Publication

Journal Publications

1. Fahim Aziz Umrani, T. O'Farrell, and Abdul Waheed, "Performance Analysis of PDC-OCDMA System with APD Mismatch", Communications in Computer and Information Science Springer-Verlag, pp 306 – 313, Vol. 20.

Submitted

2. Fahim Aziz Umrani, S. S. A. Obayya, "New Encoder/Decoder design for Spectral Amplitude Coding based OCDM system with Common Zero Code" submitted in the journal of Laser Physics Letters.

3. Fahim Aziz Umrani, S. S. A. Obayya, "Compact En/Decoder design for Spectral Amplitude Coding-OCDM System based on Perfect Difference Codes" to be submitted in IEEE journal of Lightwave technology.

4. Fahim Aziz Umrani, S. S. A. Obayya, "Manchester-Coded Modified-Legendre Codes for Spectral-amplitude Coding based optical code-division multiplexing system" submitted in the IEE Optoelectronics.

5. Fahim Aziz Umrani, S. S. A. Obayya, "Application of Perfect Difference Codes in Wireless Infrared Systems" submitted in the Intl. J. of Communications, Network and Systems Sciences.

Conference Publications

6. Fahim Aziz Umrani, S. S. A. Obayya, "Compact Encoder design for Spectral-Amplitude Coding based Optical CDMA Systems", Semiconductor & Integrated Optoelectronics Conference (SIOE'09), 6 – 8 Apr 2009, University of Cardiff, UK.

7. Fahim Aziz Umrani, S. S. A. Obayya, "Performance Analysis of Perfect Difference Codes based SAC-OCDMA System", 4th Research Student Workshop, 12 Mar 2009, Glamorgan Business Center, UK.

8. Fahim Aziz Umrani, T. O'Farrell, S. Iezekiel, and I. Robertson "Impact of APD Mismatch in Optical Code Division Multiple Access Systems using Perfect Difference Codes", London Communication Symposium 2006, United Kingdom.

9. Fahim Aziz Umrani, S. S. A. Obayya, "A Novel Spreading Sequence for Code-Division Multiplexing Systems", accepted in Semiconductor & Integrated Optoelectronics Conference (SIOE'10), Cardiff, UK.

10. Fahim Aziz Umrani, S. S. A. Obayya, "Applications of Perfect Difference Codes in Wireless Infrared Systems", poster accepted in Semiconductor & Integrated Optoelectronics Conference (SIOE'10), Cardiff, UK.